The petrosal and bony labyrinth of extinct horses (Perissodactyla, Equidae) and their implications for perissodactyl evolution (#116824)

First submission

Guidance from your Editor

Please submit by **15 May 2025** for the benefit of the authors (and your token reward) .

Structure and Criteria
Please read the 'Structure and Criteria' page for guidance.

Raw data check
Review the raw data.

Image check
Check that figures and images have not been inappropriately manipulated.

If this article is published your review will be made public. You can choose whether to sign your review. If uploading a PDF please remove any identifiable information (if you want to remain anonymous).

Files
Download and review all files from the materials page.

14 Figure file(s)
1 Table file(s)
1 Raw data file(s)

Structure and Criteria

Structure your review

The review form is divided into 5 sections. Please consider these when composing your review:

1. **BASIC REPORTING**
2. **EXPERIMENTAL DESIGN**
3. **VALIDITY OF THE FINDINGS**
4. General comments
5. Confidential notes to the editor

You can also annotate this PDF and upload it as part of your review

When ready submit online.

Editorial Criteria

Use these criteria points to structure your review. The full detailed editorial criteria is on your guidance page.

BASIC REPORTING

- Clear, unambiguous, professional English language used throughout.
- Intro & background to show context. Literature well referenced & relevant.
- Structure conforms to PeerJ standards, discipline norm, or improved for clarity.
- Figures are relevant, high quality, well labelled & described.
- Raw data supplied (see PeerJ policy).

EXPERIMENTAL DESIGN

- Original primary research within Scope of the journal.
- Research question well defined, relevant & meaningful. It is stated how the research fills an identified knowledge gap.
- Rigorous investigation performed to a high technical & ethical standard.
- Methods described with sufficient detail & information to replicate.

VALIDITY OF THE FINDINGS

- **Impact and novelty is not assessed.** Meaningful replication encouraged where rationale & benefit to literature is clearly stated.
- All underlying data have been provided; they are robust, statistically sound, & controlled.
- Conclusions are well stated, linked to original research question & limited to supporting results.

Standout reviewing tips

The best reviewers use these techniques

Tip	*Example*
Support criticisms with evidence from the text or from other sources	*Smith et al (J of Methodology, 2005, V3, pp 123) have shown that the analysis you use in Lines 241-250 is not the most appropriate for this situation. Please explain why you used this method.*
Give specific suggestions on how to improve the manuscript	*Your introduction needs more detail. I suggest that you improve the description at lines 57- 86 to provide more justification for your study (specifically, you should expand upon the knowledge gap being filled).*
Comment on language and grammar issues	*The English language should be improved to ensure that an international audience can clearly understand your text. Some examples where the language could be improved include lines 23, 77, 121, 128 – the current phrasing makes comprehension difficult. I suggest you have a colleague who is proficient in English and familiar with the subject matter review your manuscript, or contact a professional editing service.*
Organize by importance of the issues, and number your points	*1. Your most important issue* *2. The next most important item* *3. …* *4. The least important points*
Please provide constructive criticism, and avoid personal opinions	*I thank you for providing the raw data, however your supplemental files need more descriptive metadata identifiers to be useful to future readers. Although your results are compelling, the data analysis should be improved in the following ways: AA, BB, CC*
Comment on strengths (as well as weaknesses) of the manuscript	*I commend the authors for their extensive data set, compiled over many years of detailed fieldwork. In addition, the manuscript is clearly written in professional, unambiguous language. If there is a weakness, it is in the statistical analysis (as I have noted above) which should be improved upon before Acceptance.*

The petrosal and bony labyrinth of extinct horses (Perissodactyla, Equidae) and their implications for perissodactyl evolution

Owen Axel Goodchild [1], **Sydney Nicole Rosen** [2], **Bastien Mennecart** [3], **Jin Meng** [4], **Jérémy Tissier** [Corresp. 4, 5]

[1] Richard Gilder Graduate School, American Museum of Natural History, New York, New York, United States

[2] Department of Biological Sciences, Vanderbilt University, Nashville, Tennessee, United States

[3] Naturhistorisches Museum Basel, Basel, Switzerland

[4] Department of Vertebrate Paleontology, American Museum of Natural History, New York, New York, United States

[5] Palaeobiosphere Evolution Unit, Royal Belgian Institute of Natural Sciences, Brussells, Belgium

Corresponding Author: Jérémy Tissier
Email address: jeremy.tissier123@gmail.com

Perissodactyla, or odd-toed ungulates, are represented today by 16 species of rhinos, tapirs, and horses. Perissodactyls were much more diverse in the past, having a rich fossil record spanning from the earliest Eocene (~56 ma) to recent including a myriad of extinct lineages. Despite over a century of study, the inter-relationships of some extinct perissodactyl families remain poorly resolved. New morphological characters are needed to help solve this issue. Recent studies suggest that the ear region, i.e. the petrosal and the bony labyrinth of the inner ear, is a valuable source of morphological characters for mammalian phylogenetic analyses. The petrosal is the bony structure protecting the inner ear, the organs of hearing and balance in mammals. However, perissodactyl petrosals are poorly documented and have not been used in such a phylogenetic frame. In this study, we describe the petrosals and inner ears of five European fossil equid taxa and perform a preliminary phylogenetic analysis. Despite its small sample size, our phylogenetic tree recovers important groupings, which suggests the petrosal is phylogenetically informative in equids. This study supports the relevance of the ear region for phylogeny and its potential to better resolve long-contentious relationships within Perissodactyla.

The petrosal and bony labyrinth of extinct horses (Perissodactyla, Equidae) and their implications for perissodactyl evolution.

Owen Axel Goodchild[1], Sydney Nicole Rosen[2], Bastien Mennecart[3], Jin Meng[4] & Jérémy Tissier[4,5]

[1] Richard Gilder Graduate School, American Museum of Natural History, New York, New York, USA
[2] Department of Biological Sciences, Vanderbilt University, Nashville, Tennessee, USA
[3] Naturhistorisches Museum Basel, Basel, Switzerland
[4] Department of Vertebrate Paleontology, American Museum of Natural History, New York, New York, USA
[5] Palaeobiosphere Evolution Unit, Royal Belgian Institute of Natural Sciences, Brussels, Belgium

Corresponding Author:
Jeremy Tissier
Rue Vautier 29, Brussels, 1000, Belgium
Email address: jeremy.tissier123@gmail.com

Abstract

Perissodactyla, or odd-toed ungulates, are represented today by 16 species of rhinos, tapirs, and horses. Perissodactyls were much more diverse in the past, having a rich fossil record spanning from the earliest Eocene (~56 ma) to recent including a myriad of extinct lineages. Despite over a century of study, the inter-relationships of some extinct perissodactyl families remain poorly resolved. New morphological characters are needed to help solve this issue. Recent studies suggest that the ear region, i.e. the petrosal and the bony labyrinth of the inner ear, is a valuable source of morphological characters for mammalian phylogenetic analyses. The petrosal is the bony structure protecting the inner ear, the organs of hearing and balance in mammals. However, perissodactyl petrosals are poorly documented and have not been used in such a phylogenetic frame. In this study, we describe the petrosals and inner ears of five European fossil equid taxa and perform a preliminary phylogenetic analysis. Despite its small sample size, our phylogenetic tree recovers important groupings, which suggests the petrosal is phylogenetically informative in equids. This study supports the relevance of the ear region for phylogeny and its potential to better resolve long-contentious relationships within Perissodactyla.

Introduction

Today, Perissodactyla Owen 1848, also known as odd-toed ungulates, are represented by 16 living species of rhinoceroses (n5), tapirs (n4), and horses (n7). Perissodactyls have a rich fossil history extending to the early Eocene ~56 million years ago (Ma; Bai, Wang & Meng, 2018). In addition to the ancestors of living perissodactyl groups, the perissodactyl fossil record contains several totally extinct families like the clawed Chalicotheriidae or bony-horned Brontotheriidae (Bai, Wang & Meng, 2018). Despite over a century of study, the interrelationships between extinct perissodactyl families and the relationships within those families remain controversial. Phylogenetic analyses using craniodental characters have longstanding issues, such as the internal relationships of Rhinocerotoidea (Tissier et al., 2018; Bai et al., 2020).

The discordance between authors highlights the necessity to investigate other structures of perissodactyl anatomy for new phylogenetically relevant characters. The petrosal is the paired basicranial bone housing the organs of balance (semicircular canals) and hearing (cochleae) alongside their associated tissues in mammals (O'leary, 2010). Among other placental mammals, the petrosal and bony labyrinth are increasingly used in phylogenetic analyses and in understanding the paleobiology of these animals (Mennecart & Costeur, 2016; Mennecart et al., 2016; Aguirre-Fernández et al., 2017; Costeur et al., 2017; Costeur et al., 2018b; Costeur et al., 2018a; Aiglstorfer et al., 2017; Benoit et al., 2020; Mennecart et al., 2020; Evin et al., 2022; Wang et al., 2022; Mennecart et al., 2022; Orliac et al., 2023; Zhang & Tong, 2024). The petrosal and bony labyrinth have historically been a challenge to study because the bony

labyrinth is completely enclosed. Computed Tomography (CT) allows for the visualization of internal details of the petrosal and the generation of endocasts of the bony labyrinth within. The petrosal of perissodactyls is relatively poorly known and has yet to be used in large-scale phylogenetic analyses (see Mateus, 2018 for a review).

This study aims to describe the petrosal, bony labyrinth, and stapes (when preserved) of four different extinct equids, explore their morphological variations, and assess whether the petrosal characters of O'Leary (2010) and Mateus (2018) are phylogenetically informative in these taxa.

Materials & Methods

Taxonomy and specimens

This study involves seven petrosal specimens (Tab. 1; Fig. 1) from five European fossil equids housed in the collections of the Natural History Museum of Basel, Switzerland (NMB). *Anchitherium aurelianense* Cuvier, 1825 is the oldest and most basal equid in our study (Agustí & Antón, 2002), whose petrosal imaged here comes from the famous Middle Miocene locality of Sansan dated from around 15 Ma (Alberdi, Ginsburg & Rodríguez, 2004). *Hipparion* belongs to a large group of fossil equids, the Hipparionini, from across North America, Asia, Europe, and Africa (Bernor et al., 2021). The two *Hipparion* specimens come from two different sites: Montredon (Vallesian, 11-9 Ma; France) and Concud (upper Turolian, ~5 Ma, Spain; Forstén, 1982). All the *Equus* material in our sample comes from the Early Pleistocene (Villafranchian), one from Valdarno (Italy) and three from Senèze (France). They belong to the stenonine lineage that consists of Early Pleistocene European and African *Equus* (Cirilli et al., 2021a). The specimen from Valdarno belongs to *Equus stenonis,* while the specimens from Senèze belong to *Equus senezensis* (Cirilli et al., 2021b). For comparative purposes, we also included the petrosal of *Equus ferus przewalskii*, the only extant wild caballine, as described in Danilo et al. (2015). We also had access to the petrosals of *Equus caballus* (AMNH FM 118) and *Tapirus terrestris* (AMNH FM 14103) described by O'Leary (2010) for comparison.

Table 1.

Figure 1.

CT scans and segmentation

The equid material for this project was scanned at the Biomaterials Science Centre of the University of Basel, Switzerland, using a Phoenix Nanotom, GE. Tomograms were segmented using 3D Slicer (Fedorov et al., 2012) to extract the petrosal, the digital endocast of the bony labyrinth and the stapes. 3D models representing seven petrosal bones, six bony labyrinths, and three stapes were generated in 3D slicer. All tomograms and 3D models of petrosals, bony labyrinths, and

stapes are available for download on Morphosource (temporary access link for peer-review: https://www.morphosource.org/projects/000720375/temporary_link/arhmYU7XGzExNGzjpvxn1kcs?locale=en).

Measurements

Measurements were digitally performed using MeshLab2022.02 (Cignoni et al., 2008). The measurements taken included the height and width of the cochlea used for the calculation of the aspect ratio and the height, width, and length of the semicircular canal used for the calculation of the radius of curvature.

Character scores and phylogenetic analysis

We constructed a character matrix in Mesquite, combining characters from the petrosal and bony labyrinth, which is provided in Nexus format in supplemental file 1. We scored the 3D models of the petrosal and stapes with characters from Spaulding et al. (2009; available in morphobank: http://dx.doi.org/10.7934/X188). We retained the first 34 characters, which exclusively concern the petrosal bone, and the two characters of the stapes (characters 65 and 66 of Spaulding et al. 2009). We excluded characters from the auditory bulla, which was not preserved in our fossil specimens. We added 9 characters from Mateus (2018) for a total of 44 petrosal characters. We scored the 3D models of the bony labyrinth according to the 6 discrete characters of Ekdale (2013; available in morphobank: http://dx.doi.org/10.7934/X1905). We scored *Equus przewalskii* in the matrix based on the descriptions and figures of Danilo et al. (2015) and used the original scores of *Hyopsodus*, *Tapirus terrestris*, and *Equus caballus* from Spaulding et al. (2009) as well as those of *Equus* from the matrix of Ekdale (2013) and of *Hyopsodus* and *Tapirus terrestris* from Mateus (2018). In total, our matrix includes 51 characters and 10 terminals.

We performed a maximum parsimony (MP) analysis using PAUP4 (Swofford, 2002). Given the small number of taxa in our sample, we used the exhaustive search function to search all possible tree topologies to obtain the most parsimonious tree.

Anatomical terminology

The anatomical terminology used for the description of the stapes follows Orliac and Billet (2016). The terminology used for the petrosal follows O'Leary (2010) and the terminology of the inner ear follows Ekdale (2013).

Biostratigraphy

The stratigraphical framework is based on the geological timescales and European Land Mammal Ages (ELMA) for the Neogene (Raffi et al. 2020).

Results

Systematic Paleontology

Mammalia, Linnaeus 1758

Perissodactyla, Owen 1848

Equidae, Gray 1821
Anchitheriinae, Leidy 1869
Anchitherium, Meyer 1844
Anchitherium aurelianense, Cuvier 1825

Material

An isolated right petrosal, NMB.San.15063

Locality and age

Sansan, Gers, France; Miocene, Astaracian (MN 6)

Description and comparison. The petrosal of *Anchitherium aurelianense* (NMB.San.15063; Fig. 2) is 2.11 cm long anteroposteriorly. The specimen is largely complete, with minor damage to the mastoid region. The bony labyrinth could not be segmented in this specimen due to the absence of contrast between the sediment infilling the bony labyrinth and the petrosal bone.

The petrosal of *A. aurelianense* is markedly different in several aspects from that of *Equus caballus* (O'Leary 2010). In anterior view (Fig. 2C), A. *aurelianense* lacks the endocranial projection of the superiormost aspect of the petrosal seen in *Equus*. The *crista interfenestralis* is broader and more rounded than in *E. caballus*. The epitympanic wing is small, forming a low protrusion from the promontorium. The wing is rounded rather than pointed and does not protrude. The subarcuate fossa is very shallow. The opening for the *hiatus fallopii* is much larger than in *E. caballus* and is open in ventrolateral view (Fig. 2A). The opening of the *hiatus falopii* is confluent with the foramen *acousticum superius* in dorsomedial view (Fig. 2D) due to the partly broken thin wall of the secondary facial foramen. An anterior hole of the *hiatus fallopii* is also present (Fig. 2B). The stapedial muscle fossa is oval-shaped and located in the facial *sulcus*, below the *crista interfenestralis* separating the fenestra vestibule and cochleae. The fenestra cochleae is round, while the vestibular is oval. *Anchitherium* possesses a notably smaller *tegmen tympani*. Unlike in *E. caballus*, the *tegmen tympani* is flattened and is not prominent in dorsolateral view (Fig. 2B). The surface of the *tegmen tympani* is smooth, forming an angled surface anteromedially to the mastoid region. The *tegmen tympani* lacks raised bumps and the large *hiatus fallopii* opening excavates a portion of its medial edge.

The peculiar nature of the *tegmen tympani* in the petrosal of *Anchitherium* recalls the “uninflated” condition seen in the early diverging eutherians like *Protungulatum.* As in *Protungulatum*, the *tegmen tympani* is flat in *Anchitherium*. The surface is moderately raised in dorsomedial view relative to the internal acoustic meatus, while in *Protungulatum* the *tegmen tympani* is flatter in dorsomedial view. The *tegmen tympani* morphology of *Anchitherium* is somewhat intermediate between the uninflated *tegmen tympani* of *Protungulatum* and the smaller but inflated *tegmen* of *Hipparion*. It is puzzling then, that the literature reports the earlier diverging equid *Orohippus* with an inflated *tegmen tympani* (Cifelli, 1982). Indeed, all the fossil tapirs Mateus (2018)

referred to have an inflated tegmen tympani. See the discussion for further consideration.

A. aurelianense lacks an anterior process of the *tegmen tympani*. A ventrolateral tuberosity was present in *A. aurelianense*. Medial to the external acoustic meatus is a relatively deep epitympanic recess. *A. aurelianense* lacks a distinct stylomastoid notch.

The petrosal is narrow in ventromedial view (Fig. 2E), widening into a fan-shaped mastoid region like in *E. caballus* (O'Leary, 2010). The mastoid region is very incomplete. It was considered here to be large as per O'Leary 2010's definition but is notably smaller than that of *E. caballus*.

The mastoid process is absent in *Anchitherium*, the preserved element of the mastoid is consistent with a wedge shape as described in O'Leary (2010).

Figure 2.

Equinae, Steinmann and Döderlein 1890
Hipparionini, Quin 1955
Hipparion, Christol 1832
Hipparion depereti, Sondaar 1974

Material

An isolated left petrosal, NMB.A.Mo655

Locality and age

Montredon, France; Late Miocene Vallesian (MN 10).

Description and comparison. The Montredon *Hipparion*, *Hipparion depereti*, specimen NMB.A.Mo655, is a largely complete petrosal, with minor damage to the tegmen tympani and the mastoid region. Segmentation of its bony labyrinth was made challenging by the presence of very dense infilling (possibly iron). NMB.A.Mo.655 is an isolated petrosal measuring 3.9 cm in length. This petrosal is intermediate between *Anchitherium* and *Equus*. Notably, the petrosal of *H. depereti* is more massively constructed and broader than that of *Anchitherium aurelianense*. There are notable distinctions from *Equus*, however. The *promontorium* gives rise to the epitympanic wing (Fig. 3B), which is small and rounded rather than pointed as in *E. caballus* (O'Leary, 2010), but longer than in *Anchitherium*.

Between the epitympanic wing and the *tegmen tympani* lies the opening for the *hiatus Fallopii*, which is smaller in *Hipparion depereti* than in *Anchitherium* but larger than in *E. caballus* (O'Leary, 2010). The *hiatus Fallopii* is directly confluent with the foramen *acousticum superius*. The fossa for the *tensor tympani* is located between the *hiatus Fallopii* and the fenestra vestibule. The stapedial muscle fossa is deep and round in the facial sulcus, just below the crista interfenestralis. The *tegmen tympani* (Fig. 3C, D) is more greatly inflated than in *A. aurelianense* but much less than in *E. caballus*.

There is no anterior process of the *tegmen tympani*. In dorsomedial view (Fig. 3E), the surface of the area around the internal acoustic meatus is smooth. However, this specimen has been abraded, making the surface appear more rugose than in life. The subarcuate fossa is wide and shallow, as in *E. caballus* (O'Leary, 2010). In dorsolateral view (Fig. 3C), the ventromedial surface of the petrosal is narrow anteriorly and expands into a fan-shaped mastoid region posteriorly. The medial surface of the petrosal is flat. The basicapsular groove can be seen along the dorsal margin of the petrosal (Fig. 3F). The cochlear aqueduct is a very small hole at the ventromedial margin (Fig. 3E-F), although located more ventrally than in *Tapirus terrestris* (like *E. caballus*). The mastoid is incomplete, with the ventral knob-like area well-preserved, but lacking the dorsal point seen in *E. caballus* (O'Leary, 2010).

Figure 3.

The bony labyrinth of NMB.A.Mo.655 is more poorly preserved than the other specimens in this study, as dense infilling obscured the shape of the semicircular canals. Nevertheless, the gross morphology of the bony labyrinth can be described and discussed. It shows little post-mortem deformation. The bony labyrinth fills much of the volume of the petrosal, but not to the extent observed in *Hyopsodus lepidus* (Ravel & Orliac, 2015). The secondary bony lamina was not observed. This may be due to poor preservation, or a genuine absence. In the bony labyrinth of the earlier diverging equid *Xenicohippus osborni* no secondary bony lamina was observed, although deformation made that observation questionable (Ravel & Orliac, 2015). In the more derived *E. caballus*, the secondary bony lamina is weakly developed (Ekdale, 2013). The cochlear spiral is like that of *E. caballus*, here considered high, although notably lower than that observed in *Hyopsodus lepidus* (Ravel & Orliac, 2015). The cochlea completes two and a half turns and is loosely coiled like *E. caballus* (Ekdale, 2013). As in *X. osborni*, the cochlea is elliptical, with the anteroposterior axis longer than the mediolateral axis. The cochlear aqueduct is straight, narrowing as it nears its external aperture as in *E. caballus* (Ekdale, 2013), and short. The posterior entry of the lateral semicircular canal is through the posterior ampulla, as in *E. caballus* (Ekdale, 2013). Like both *X. osborni* and *E. caballus*, the arc of the anterior semicircular canal possesses the largest radius and the greatest height of the three (Ravel & Orliac, 2015). The lateral semicircular canal sits higher than the posterior semicircular canal. The posterior and lateral semi-circular canals lay at a right angle to one another (Fig. 4C), while the angle between the posterior and anterior canal is slightly obtuse (Fig. 4D). Anterior and posterior canals are relatively rounded, while the lateral one is ovoid in shape. All the canals are thick in section. The long endolymphatic sac is triangular in shape and posteriorly projected. It starts high, almost at the dorsal end of the common crus. The shape of the fenestrae cannot be described due to preservation. There is no clear distinction between the

vestibula and the cochlea, maybe due to the preservation of the specimen. The cochlea is detached from the vestibula.

Figure 4.

Hipparion concudense, Pirlot 1956

Material

An isolated left petrosal, NMB.Ccd.3

Locality and age

Concud 3, Teruel, Spain; Late Miocene, Turolian (MN 12).

Description and comparison. The Concud 3 *Hipparion*, *Hipparion concudense*, specimen is an almost entirely complete petrosal, with only minor damage to the mastoid region. The Concud 3 *Hipparion* preserved a stapes within the bony labyrinth *Hipparion concudense* is represented by an isolated petrosal measuring 3.15 cm in length. The petrosal of *H. concudense* is similar in most aspects to its geologically older relative *H. depereti*. The epitympanic wing is a low-rounded structure protruding gently from the anterior portion of the promontorium. The caudal tympanic process, located posterior to the fenestra cochlae, is mediolaterally broad but not to the same extent observed in *E. caballus* (O'Leary, 2010). The mastoid region is large, occupying about half the size of the bone. As in both fossil and extant equids, the mastoid is irregularly shaped with a knobby surface. Likewise, as in the other fossil equids described here, the long mastoid process is absent, leaving only the fan-like proximal portion of the mastoid. The mastoid of *H. concudense* is not as greatly expanded as that of *H. depereti*. The thin bony lamina that covers the *hiatus Fallopii* is still preserved and separates the secondary facial foramen from the anterior hole of the *hiatus Fallopii* (Fig. 5B). The stapedial muscle fossa is extremely deep, large and oval-shaped, although this may be related to allometry. The facial sulcus is deep.

In dorsomedial view (Fig. 5E), the *tegmen tympani* is markedly smaller than *E. caballu*s, though slightly inflated laterally. The *tegmen tympani* has a flat surface and lacks the large anterior process seen on *E. caballus* (O'Leary, 2010). The basicapsular groove sits along the dorsal edge of the petrosal (Fig. 5D), and the cochlear aqueduct (Fig. 5E-F) sits in a slit situated more ventrally than ventromedially as in *E. caballus* (O'Leary, 2010). In the anterior view (Fig. 5D), the superiormost portion of the petrosal does not project medially, at least not to the extent seen in *E. caballus* (O'Leary, 2010).

Figure 5.

The bony labyrinth of *Hipparion concudense* is better preserved than that of *H. depereti*. Like NMB.A.Mo.655, it shows little post-mortem deformation to the structure of the semicircular canals. The secondary bony lamina is here observed. The cochlea

forms a loose spiral of 2.5 turns like both *H. depereti* and *E. caballus* (Ekdale, 2013). The cochlear aqueduct narrows as it nears the aperture, as observed in *H. depereti*. The anterior semicircular canal has both the greatest height and radius of curvature. Like both, *H. depereti* and *E. caballus,* the posterior entry of the lateral semicircular canal is through the posterior ampulla, and the lateral semicircular canal sits higher than the posterior semicircular canal. The angle between the posterior and anterior canal (Fig. 6D) is more obtuse than in *Hipparion depereti*. It also differs from *Hipparion depereti* by its more posteriorly elongated lateral canal in dorsal view (Fig. 6D). The anterior canal is more rounded than the posterior one. The lateral one is ovoid in shape with a clear narrowing of the ellipse. All the canals are relatively thin in section. The long endolymphatic sac is triangular in shape and posteriorly projected. It starts below the common crus, in its axis. There is a hinge between the vestibula and the cochlea. The cochlea is few detached from the vestibula.

The stapes of *H. concudense* (Fig. 7A) was preserved inside the vestibule of the bony labyrinth, which happens occasionally, as reported by Orliac and Billet (2016). It seems to be broken or poorly preserved, lacking most of its medial side (Fig. 7A). The overall general shape is quite similar to that of *Equus caballus* illustrated by Doran (1878: pl. 61, fig. 3). In lateral view, the foramen intercrurale is large and rectangular. The *capitulum* cannot be distinguished from the rest of the body of the stapes or is not preserved. The *basis stapedis* is oval-shaped.

Figure 6.

Figure 7.

Equini Quinn 1955

Equus Linnaeus 1758

Equus stenonis Cocchi 1867

Material

An isolated left petrosal, NMB.V.A.2753

Locality and Age

Valdarno, Italy; Early Pleistocene, Villafranchian age (MNQ 18).

Description and comparison. *Equus stenonis* from Valdarno is represented by an isolated petrosal (NMB.V.A.2753) measuring 3.55 cm in length. The petrosal is well preserved, with the only major damage being to the mastoid process. The Valdarno *Equus* preserved a stapes within the bony labyrinth. In overall character, it is strikingly more similar to *E. caballus* (O'Leary, 2010) and *E. senezensis* than to *Hipparion* and especially *Anchitherium*. *E. stenonis* and *E. senezensis* are similar to *E. caballus* in possessing a prominent anterior projection of the tegmen tympani, while *Hipparion* and *Anchitherium* have low tegmen tympani lacking such pronounced anterior projections. The tegmen tympani has a prominent anterior process ending in a point, as in *E.*

caballus (O'Leary, 2010). The anterior process of the tegmen tympani of *Equus stenonis* does not extend anterior to the promontorium. The caudal tympanic process is wide and smooth, with an expansion similar to extant *E. caballus* rather than *Hipparion* or *Anchitherium*. The mastoid region is large, and as in the other fossil equids the broad proximal area is preserved but not the elongate mastoid process. The subarcuate fossa is wide and shallow as in *E. caballus* (O'Leary, 2010). The surface of the mastoid is knobby and irregular like that of *E. caballus.* The mastoid meets and joins the caudal tympanic process such that the mastoid juts out at an angle when viewed in ventrolateral view. Two grooves along the ventromedial edge of the bone demarcate the basicapsular groove, with the cochlear aqueduct laying at the posterior edge of this groove. The ventrolateral side (Fig. 8E) is not very well preserved, and the segmentation of this area was difficult due to the preservation of the bulla, which we excluded in the figures. The *hiatus fallopii* is wide open and opens directly into the foramen *acousticum superius*. The facial *sulcus* is barely visible and quite shallow. The petrosal is narrow in ventromedial view (Fig. 8F), expanding into a fan-shaped mastoid process.

Figure 8.

The bony labyrinth of *Equus stenonis* is nearly identical to *E. caballus* (Ekdale, 2013). The cochlea is loosely coiled forming 2.5 turns. The cochlea takes on an elliptical shape, longer anteroposteriorly than mediolaterally. Like *E. caballus* the posterior entry of the lateral semicircular canal is through the posterior ampulla, the largest semicircular arc radius of curvature is in the anterior semicircular canal, and the lateral semicircular canal sits higher than the posterior semicircular canal. The posterior ampulla is larger than in *Hipparion* (Fig. 9B-C). However, the anterior canal seems to be more elliptic than the posterior one due to a straight projection of the canal when connecting with the common crus. The lateral one is slightly ovoid in shape but larger than in *H. concudense*. All the canal are relatively thin in section. The small endolymphatic sac is triangular in shape and posteriorly projected, not in line with the common crus. It starts close to the base of the common crus due to a very short and posteriorly projected vestibular aqueduct. There is a hinge between the vestibula and the cochlea. The cochlea is few detached from the vestibula.

The stapes of *Equus stenonis* (Fig. 7B) is very similar to that of *H. concudense*, but it is more complete. The foramen *intercrurale* is larger on the lateral side than medial, as observed in some artiodactyls (Orliac and Billet 2016). The *basis stapedis* is oval-shaped (Fig. 7B). In medial and lateral views (Fig. 7B), the stapes is roughly triangular. The *capitulum stapedis* cannot be differentiated from the rest of the body of the stapes. In medial view, the *foramen intercrurale* is much smaller than on the lateral side.

Figure 9.

Equus senezensis, Azzaroli 1964

Material

Three petrosals, including the left and right petrosals and one stapes of a single individual (NMB.Se.141) and an isolated left petrosal (NMB.Se.554).

Locality and Age

Seneze, France; Early Pleistocene, Villafranchian (MNQ 18).

Description & comparison. *Equus senezensis* was represented by three petrosals, two of which represent the left and right petrosals of a single individual NMB.Se.141, and one from NMB.Se.554. The petrosals vary in size from 3.60 to 3.94 cm anteroposteriorly. They differ from that of *Equus caballus* (O'Leary, 2010) in several ways. Between the *fenestra cochleae* and the *fenestra vestibuli* is a *crista interfenestralis* that is pronounced but not as sharp in comparison to *E. caballus* (O'Leary, 2010). The fossa for *tensor tympani* is a large, oval, and deep depression (Fig. 10D). It significantly excavates the surrounding *tegmen tympani*. The epitympanic wing is present and protrudes from the promontory but is very small. There is a distinct anterior hole for the *hiatus Fallopii* and it is relatively large (Fig. 10B). A posteromedial flange extends from the *promontorium* such that the *promontorium* is surrounded by a complete, flat flange of bone similar to that of *E. caballus* (O'Leary, 2010), though it appears to extend even further posteriorly. The fossa for the tensor tympani is shallow and oval (Fig. 11B). The *tegmen tympani* is flat and moderately inflated, contributing to about one-fifth the total width of the ventrolateral view though slightly more inflated than that of *E. caballus* (O'Leary, 2010). The anterior process of the tegmen tympani is larger than that of *E. caballus* and extends anterior to the promontorium before terminating in a less pronounced point (O'Leary, 2010). The mastoid region is large and wedge-shaped, irregular, and knobby, though it appears rounder than that of *E. caballus* (O'Leary, 2010). The facial sulcus and stapedial muscle fossa cannot be observed.

The ventromedial edge of the bone has a basicapsular groove, and at its posterior edge houses a small cochlear aqueduct (Fig. 11E). The slit for the cochlear aqueduct is smaller in NMB.Se.554 (Fig. 11E) than in NMB.Se.141 (Fig. 10E). In the ventromedial view, the petrosal is narrow and widens into a fan-shaped mastoid region with bumps and projections. The ventromedial surface is relatively flat (Fig. 11C). There are vascular grooves on the dorsolateral side of the *tegmen tympani* (Fig. 10C). The cochlear aqueduct is a small hole at the ventromedial margin but is found within a large slit (Fig. 10D-E).

We can observe patterns of intra-individual variation due to asymmetry in the petrosal of *Equus senezensis*. The two petrosals of NMB.Se.141 differ indeed in some respects such as the subarcuate fossa, which is smaller in the right petrosal than in the

left one. Such variation is consistent with Danilo et al (2015)'s study of modern *Equus,* where the size, morphology, elongation, and depth of the subarcuate fossa can be highly variable among individuals.

Figure 10.

Figure 11.

The basal portion of the cochlear coil of *Equus senezensis* (NMB.Se.141 and NMB.Se.554; Fig. 12-13) begins slightly straight before forming a pronounced curve that becomes the spiral shape of the cochlea detaching the cochlea from the vestibula. The latter part of the coil begins as a loose spiral that becomes tighter towards the apex. The coil remains tightly wound consistently after about the first quarter of the first basal turn. The cochlea completes about 2.5 turns and is more tightly coiled compared to *Equus caballus* (Ekdale, 2013). The left cochlea of *Equus senezensis* has a high aspect ratio of 0.65 to 0.82 in contrast to the low aspect ratio of *E. caballus* (0.41; Ekdale 2013, tab. 2).

NMB.Se.554 has the spherical and elliptical recesses separated by a constriction of the vestibule that forms a bony ring. This condition is observed in both *E. caballus* (Ekdale, 2013) and *E. senezensis* but is more pronounced in this individual than in NMB.Se.141. The entry of the lateral semicircular canal into the posterior one is through the posterior ampulla. The bony ring is quite pronounced and nearly parallel to the plane of the lateral semicircular canal. However, the posterior canal seems to be more elliptic than the anterior one due to a straight projection of the canal when connecting with the common crus. The lateral one is relatively rounded. All the canals are relatively thin in section. The large endolymphatic sac is rectangular in shape and posteriorly projected, not in line with the common crus. It starts almost at mid-height of the common crus due to a slightly posteriorly projected vestibular aqueduct. There is a hinge between the vestibula and the cochlea. The cochlea is few detached from the vestibula.

Figure 12.

Figure 13.

The stapes of *Equus senezensis* was preserved inside the vestibule of the left petrosal NMB.Se.141 (Fig. 7C). It is overall quite similar to *Equus caballus* (Doran 1878), or the other two stapes described here, but is not well preserved. The *processus muscularis stapedis* is difficult to identify, but seems to be visible on the posterolateral face of the stapes (Fig. 7C). As in the other species, the *foramen intercrurale* is smaller on the medial side than on the lateral side. The *capitulum* cannot be identified.

Preliminary Phylogenetic Analysis

Using our combined dataset (see Material and Methods), we obtained a single most-parsimonious tree of 25 steps (Fig. 14), with a consistency index (CI) of 0.88, a retention index (RI) of 0.82, and a homoplasy index (HI) of 0.12. Of the 51 characters in the analysis, 29 are constant and only 10 are parsimony informative. The clade Equidae is supported by five synapomorphies in ACCTRAN optimization:

- the absence of anterior process of the *tegmen tympani*,
- the apex of the anterior process of the *tegmen tympani* pointed when present,
- the lateral semicircular canal higher than the posterior,
- the cochlear spiral high,
- and the cochlear aqueduct is in the ventral face.

The clade Equinae is supported by four synapomorphies:

- the presence of the ventrolateral tuberosity of the petrosal,
- the pars cochlearis protrudes ventromedially,
- the caudal tympanic process long,
- and the subarcuate fossa wide.

None of the Equinae have autapomorphies, whereas *Anchitherium* has three. *Equus* is monophyletic and supported by one unambiguous synapomorphy: the presence of an anterior process of the *tegmen tympani* (character 11). All perissodactyls, including *Tapirus*, differ from *Hyopsodus* by seven characters. Finally, this topology differs from the literature in recovering *E. senezensis* more closely related to extant horses (*E. caballus* and *E. przewalskii*) than to *E. stenonis* (Cirilli et al., 2021a) and by the paraphyly of *Hipparion*. In our analysis, *Hipparion concudense* differs from *H. depereti* by the absence of extension of the fossa for *tensor tympani*.

Figure 14.

Discussion

Among both extant tapirs and horses, characters of the petrosal have been observed to be individually variable. Among equids, Danilo et al. (2015) described the petrosals of 14 *Equus przewalskii* individuals of varying ages, sexes, and sizes (Danilo et al., 2015) while Costeur et al. (2017) also observed it in an ontogenetic series of *Bos*. They showed that the depth of the petrosal groove, the shape of the internal acoustic meatus, as well as the shape, size, and elongation of the subarcuate fossa were individually variable depending on the age of the individual. Mateus (2018) showed that in *Tapirus terrestris* the depth and size of the subarcuate fossa are individually variable like in *E. przewalskii* as well as the position of the caudal tympanic process and the *hiatus fallopii*. The subarcuate fossa accounted for one character in Spaulding et al., (2009) and two in Mateus (2018). All the perissodactyls in our analysis shared a deep subarcuate fossa.

Tapirus terrestris and *Anchitherium aurelianense* were both scored as small for the size of the subarcuate fossa while all the other taxa were scored as large. For all the other variable characters from Mateus (2018), every taxon in our analysis had a terminal position of the *hiatus fallopii*, and only *T. terrestris* was scored with a ventrally positioned caudal tympanic process.

We have to keep in mind that the petrosal bone, contrary to the bony labyrinth, is a structure that ossifies in parallel to the surrounding skull bones (Mennecart & Costeur 2016, Costeur et al. 2017). Then this bone may greatly suffer from allometry (ontogenic and evolutionary) complexifying the interpretation of the evolutionary polarity of the characters. On the contrary, the bony labyrinth is an organ that fully ossifies during fetus stages in placental mammals (e.g. Mennecart & Costeur 2016, Costeur et al. 2017). Shape and size remain similar during all the life of the animal, providing exceptional results considering micro-and macroevolutionary processes (Evin et al. 2022, Mennecart et al. 2022). This organ may represent a structure with a neutral evolution (Mennecart et al. 2022), where gradual changes can be observed. The ear region of extinct perissodactyls remains poorly understood, relative to artiodactyls. The petrosal of extinct perissodactyls was only described for three Equoids (Kits, 1956; Cifelli, 1982; O'Leary 2010), four tapiromorphs (Savage, et al., 1965; Radinsky & Expeditions (1921-1930), 1965; Colbert, 2006; Li and Wang, 2010; O'Leary, 2010), one brontothere (Mader, 2009), and one Ancylopod (Bai, Wang & Meng, 2010) so far. The petrosal of rhinocerotoids is especially poorly understood. O'Leary (2010) described the incomplete petrosal of *Dicerorhinus sumatrensis*, while Robert et al. (2021) investigated the petrosal and bony labyrinth of *Ceratotherium simum simum*, and Manning (1985) reported an isolated petrosal of *Metamynodon*. Moreover, recent molecular investigations have suggested that the extinct South American Native Ungulates (SANUs) were related to perissodactyls (Welker et al., 2015). Morphological phylogenies without molecular constraints have struggled to recover this result (Kramarz & Macphee, 2023). Morphological data from the petrosal and bony labyrinth of SANUs has clarified the internal relationships of SANUs (Perini et al., 2022). Comparisons between the petrosal of SANUs and other placentals has been limited thus far, and have not included perissodactyls (Billet & Muizon, 2013). The ear region' insight into phylogeny among perissodactyls may, therefore, also be key to illuminating their potential relationships to SANUs and other extinct hoofed mammal groups like phenacodontids and cambaytheres.

Conclusions

The results of our preliminary phylogenetic analyses suggest that the ear region is informative for perissodactyl phylogeny and invites future research. This limited analysis suggests that the petrosal morphology may be informative in family and genus-level cladistics, but it currently lacks precision for generic level distinctions considering its

inability to recover the monophyly of the genus *Hipparion*. Further investigation is necessary to better understand the phylogenetical interest of the selected character in regards to their allometric constrains and variation. Moreover, the bony labyrinth has been proven to be a structure that evolves mostly neutrally. Including more bony labyrinth characters, may be usefull for a better understanding of the perissodactyls evolutionary history and to obtain finer results. Obviously, a much larger sampling would be needed to fully investigate the phylogeny of Equidae or other perissodactyls, but we believe that petrosal and inner ear's morphology should be a valuable addition in future larger-scale phylogenetic analysis. Although only ten characters were here parsimony informative, we think that with a larger scale taxonomic sample, more characters would become phylogenetically informative.

Acknowledgements

This study would not have been possible without the support of Loïc Costeur (Natural History Museum of Basel), and we are thus highly indebted to him for providing access to the specimens studied here and for allowing us to CT-scan them, as a part of his project SCN125-BC funded by the Swiss Academy of Sciences (SCNAT). We are also extremely grateful to Georg Schulz (Department of Biomedical Engineering, University of Basel) for CT-scanning the specimens for us. The authors would like to thank Alana Gishlick and Ruth O'Leary (American Museum of Natural History) for access to and curation of some comparison specimens in this study. Additionally, we would like to thank R. Benjamin Sulser, John J. Flynn, Jocelyn A. Sessa, Bryce E. Koester, Jason P. Downs, and Edward "Ted" B. Daeschler for useful interactions with the authors that helped this project develop. We are very thankful for the support of the Research Experiences for Undergraduates (REU) program of the U.S. National Science Foundation for supporting O. Goodchild and S. Rosen at the American Museum of Natural History.

References

Aguirre-Fernández G, Mennecart B, Sánchez-Villagra MR, Sánchez R, Costeur L. 2017. A dolphin fossil ear bone from the northern Neotropics–insights into habitat transitions in iniid evolution. *Journal of Vertebrate Paleontology* 37:e1315817. DOI: 10.1080/02724634.2017.1315817.

584 Agustí J, Antón M. 2002. *Mammoths, sabertooths, and hominids: 65 million years of*
585 *mammalian evolution in Europe*. New York: Columbia University Press.
586 Aiglstorfer M, Costeur L, Mennecart B, Heizmann EPJ. 2017. *Micromeryx? eiselei*—A
587 new moschid species from Steinheim am Albuch, Germany, and the first
588 comprehensive description of moschid cranial material from the Miocene of
589 Central Europe. *PLOS ONE* 12:e0185679. DOI: 10.1371/journal.pone.0185679.
590 Alberdi MT, Ginsburg L, Rodríguez J. 2004. *Anchitherium aurelianense* (Mammalia,
591 Equidae) (Cuvier, 1825) dans l'Orléanien (Miocène) de France.
592 Bai B, Meng J, Zhang C, Gong Y-X, Wang Y-Q. 2020. The origin of Rhinocerotoidea
593 and phylogeny of Ceratomorpha (Mammalia, Perissodactyla). *Communications*
594 *Biology* 3:1–16. DOI: 10.1038/s42003-020-01205-8.
595 Bai B, Wang Y, Meng J. 2010. New Craniodental Materials of *Litolophus gobiensis*
596 (Perissodactyla, "Eomoropidae") from Inner Mongolia, China, and Phylogenetic
597 Analyses of Eocene Chalicotheres. *American Museum Novitates* 2010:1–27. DOI:
598 10.1206/678.1.
599 Bai B, Wang Y-Q, Meng J. 2018. The divergence and dispersal of early perissodactyls
600 as evidenced by early Eocene equids from Asia. *Communications Biology* 1:1–10.
601 DOI: 10.1038/s42003-018-0116-5.
602 Benoit J, Legendre LJ, Farke AA, Neenan JM, Mennecart B, Costeur L, Merigeaud S,
603 Manger PR. 2020. A test of the lateral semicircular canal correlation to head
604 posture, diet and other biological traits in "ungulate" mammals. *Scientific Reports*
605 10:19602. DOI: 10.1038/s41598-020-76757-0.

606 Bernor RL, Kaya F, Kaakinen A, Saarinen J, Fortelius M. 2021. Old world hipparion
607 evolution, biogeography, climatology and ecology. *Earth-Science Reviews*
608 221:103784. DOI: 10.1016/j.earscirev.2021.103784.
609 Billet G, Muizon CD. 2013. External and internal anatomy of a petrosal from the late
610 Paleocene of Itaboraí, Brazil, referred to Notoungulata (Placentalia). *Journal of*
611 *Vertebrate Paleontology* 33:455–469. DOI: 10.1080/02724634.2013.722153.
612 Cifelli RL. 1982. The Petrosal Structure of *Hyopsodus* with Respect to That of Some
613 Other Ungulates, and Its Phylogenetic Implications. *Journal of Paleontology*
614 56:795–805.
615 Cignoni P, Callieri M, Corsini M, Dellepiane M, Ganovelli F, Ranzuglia G. 2008.
616 MeshLab: an Open-Source Mesh Processing Tool.
617 Cirilli O, Pandolfi L, Rook L, Bernor RL. 2021a. Evolution of Old World *Equus* and origin
618 of the zebra-ass clade. *Scientific Reports* 11:10156. DOI: 10.1038/s41598-021-
619 89440-9.
620 Cirilli O, Saarinen J, Pandolfi L, Rook L, Bernor RL. 2021b. An updated review on
621 *Equus stenonis* (Mammalia, Perissodactyla): New implications for the European
622 early Pleistocene *Equus* taxonomy and paleoecology, and remarks on the Old
623 World *Equus* evolution. *Quaternary Science Reviews* 269:107155. DOI:
624 10.1016/j.quascirev.2021.107155.
625 Colbert MW. 2006. *Hesperaletes* (Mammalia: Perissodactyla), a new tapiroid from the
626 middle Eocene of southern California. *Journal of Vertebrate Paleontology* 26:697–
627 711. DOI: 10.1671/0272-4634(2006)26[697:HMPANT]2.0.CO;2.

628 Costeur L, Andrea V, Célia B, Mennecart B. 2018a. On some ruminant petrosal bones
629 and their bony labyrinth from Senèze (Villafranchian, France). *Revue de*
630 *Paleobiologie* 37:443–456. DOI: 10.5281/zenodo.2545101.
631 Costeur L, Grohé C, Aguirre-Fernández G, Ekdale E, Schulz G, Müller B, Mennecart B.
632 2018b. The bony labyrinth of toothed whales reflects both phylogeny and habitat
633 preferences. *Scientific Reports* 8:7841. DOI: 10.1038/s41598-018-26094-0.
634 Costeur L, Mennecart B, Müller B, Schulz G. 2017. Prenatal growth stages show the
635 development of the ruminant bony labyrinth and petrosal bone. *Journal of Anatomy*
636 230:347–353. DOI: 10.1111/joa.12549.
637 Danilo L, Remy J, Vianey-Liaud M, Mérigeaud S, Lihoreau F. 2015. Intraspecific
638 Variation of Endocranial Structures in Extant Equus: A Prelude to Endocranial
639 Studies in Fossil Equoids. *Journal of Mammalian Evolution* 22:561–582. DOI:
640 10.1007/s10914-015-9293-x.
641 Doran, A. H. 1878. XVIII. Morphology of the mammalian Ossicula auditûs. *Transactions*
642 *of the Linnean Society of London. 2nd Series. Zoology*, *1*(7), 371-497.
643 Ekdale EG. 2013. Comparative Anatomy of the Bony Labyrinth (Inner Ear) of Placental
644 Mammals. *PLOS ONE* 8:e66624. DOI: 10.1371/journal.pone.0066624.
645 Evin A, David L, Souron A, Mennecart B, Orliac M, Lebrun R. 2022. Size and shape of
646 the semicircular canal of the inner ear: A new marker of pig domestication?
647 *Journal of Experimental Zoology Part B: Molecular and Developmental Evolution*
648 338:552–560. DOI: 10.1002/jez.b.23127.
649 Fedorov A, Beichel R, Kalpathy-Cramer J, Finet J, Fillion-Robin J-C, Pujol S, Bauer C,
650 Jennings D, Fennessy F, Sonka M, Buatti J, Aylward S, Miller JV, Pieper S, Kikinis

651 R. 2012. 3D Slicer as an image computing platform for the Quantitative Imaging
652 Network. *Magnetic Resonance Imaging* 30:1323–1341. DOI:
653 10.1016/j.mri.2012.05.001.
654 Forstén A. 1982. *Hipparion primigenium melendezi* Alberdi reconsidered. *Annales*
655 *Zoologici Fennici* 19:109–113.
656 Kitts D. 1956. American *Hyracotherium* (Perissodactyla, Equidae). *Bulletin of the*
657 *American Museum of Natural History* 110.
658 Kramarz AG, Macphee RDE. 2023. Did some extinct South American native ungulates
659 arise from an afrothere ancestor? A critical appraisal of Avilla and Mothé's (2021)
660 Sudamericungulata – Panameridiungulata hypothesis. *Journal of Mammalian*
661 *Evolution* 30:67–77. DOI: 10.1007/s10914-022-09633-5.
662 Mader BJ. 2009. Details of the cranial anatomy of a primitive diplacodont brontothere,
663 cf. *Protitanotherium*, from the Wiggins Formation of Wyoming (Mammalia,
664 Perissodactyla, Brontotheriidae). *Journal of Vertebrate Paleontology* 29:1224–
665 1232. DOI: 10.1671/039.029.0414.
666 Manning, E. M. 1997. An early Oligocene rhinoceros jaw from the marine Byram
667 Formation of Mississippi. *Mississippi Geology*, *18*(2)..
668 Mateus, A. L. D. 2018. The anatomical description of the osseous inner ear of tapirus
669 and the evolution of the petrosal in perissodactyla. Ph.D. dissertation, Minas
670 Gerais: Universidade Federal de Minas Gerais.
671 Mennecart B, Dziomber L, Aiglstorfer M, Bibi F, DeMiguel D, Fujita M, Kubo MO,
672 Laurens F, Meng J, Métais G, Müller B, Ríos M, Rössner GE, Sánchez IM, Schulz
673 G, Wang S, Costeur L. 2022. Ruminant inner ear shape records 35 million years of

674 neutral evolution. *Nature Communications* 13:7222. DOI: 10.1038/s41467-022-
675 34656-0.
676 Mennecart B, Guignard C, Dziomber L, Schulz G, Müller B, Costeur L. 2020. Allometric
677 and Phylogenetic Aspects of Stapes Morphology in Ruminantia (Mammalia,
678 Artiodactyla). *Frontiers in Earth Science* 8. DOI: 10.3389/feart.2020.00176.
679 Mennecart B, Rössner GE, Métais G, DeMiguel D, Schulz G, Müller B, Costeur L. 2016.
680 The petrosal bone and bony labyrinth of early to middle Miocene European deer
681 (Mammalia, Cervidae) reveal their phylogeny. *Journal of Morphology* 277:1329–
682 1338. DOI: 10.1002/jmor.20579.
683 O'leary MA. 2010. An Anatomical and Phylogenetic Study of the Osteology of the
684 Petrosal of Extant and Extinct Artiodactylans (Mammalia) and Relatives. *Bulletin of*
685 *the American Museum of Natural History* 2010:1–206. DOI: 10.1206/335.1.
686 Orliac MJ, Maugoust J, Balcarcel A, Gilissen E. 2023. Paleoneurology of Artiodactyla,
687 an Overview of the Evolution of the Artiodactyl Brain. In: Dozo MT, Paulina-
688 Carabajal A, Macrini TE, Walsh S eds. *Paleoneurology of Amniotes : New*
689 *Directions in the Study of Fossil Endocasts*. Cham: Springer International
690 Publishing, 507–555. DOI: 10.1007/978-3-031-13983-3_13.
691 Perini FA, Macrini TE, Flynn JJ, Bamba K, Ni X, Croft DA, Wyss AR. 2022. Comparative
692 Endocranial Anatomy, Encephalization, and Phylogeny of Notoungulata
693 (Placentalia, Mammalia). *Journal of Mammalian Evolution* 29:369–394. DOI:
694 10.1007/s10914-021-09583-4.
695 Radinsky LB. 1965. Early Tertiary Tapiroidea of Asia. *Bulletin of the American Museum*
696 *of Natural History* 129:2.

Raffi, I., Wade, B. S., Pälike, H., Beu, A. G., Cooper, R., Crundwell, M. P., ... & Vernyhorova, Y. V. 2020. The Neogene period. In *Geologic time scale 2020* (pp. 1141-1215). Elsevier.

Ravel A, Orliac MJ. 2015. The inner ear morphology of the 'condylarthran' *Hyopsodus lepidus*. *Historical Biology* 27:957–969. DOI: 10.1080/08912963.2014.915823.

Robert MP, Carstens A, de Beer FC, Hoffman JW, Steenkamp G. 2021. Micro-anatomy of the ear of the southern white rhinoceros (*Ceratotherium simum simum*). *Anatomia, Histologia, Embryologia* 50:316–323. DOI: 10.1111/ahe.12632.

Spaulding M, O'Leary MA, Gatesy J. 2009. Relationships of Cetacea (Artiodactyla) Among Mammals: Increased Taxon Sampling Alters Interpretations of Key Fossils and Character Evolution. *PLOS ONE* 4:e7062. DOI: 10.1371/journal.pone.0007062.

Swofford D. 2002. PAUP* 4.0 : Phylogenetic Analysis Using Parsimony

Tissier, J., Becker, D., Codrea, V., Costeur, L., Fărcaş, C., Solomon, A., Venczel, M., & Maridet, O. (2018). New data on Amynodontidae (Mammalia, Perissodactyla) from Eastern Europe: Phylogenetic and palaeobiogeographic implications around the Eocene-Oligocene transition. *PLoS One*, *13*(4), e0193774.

Wang S-Q, Ye J, Meng J, Li C, Costeur L, Mennecart B, Zhang C, Zhang J, Aiglstorfer M, Wang Y, Wu Y, Wu W-Y, Deng T. 2022. Sexual selection promotes giraffoid head-neck evolution and ecological adaptation. *Science* 376:eabl8316. DOI: 10.1126/science.abl8316.

718 Welker, F., Collins, M. J., Thomas, J. A., Wadsley, M., Brace, S., Cappellini, E., ... &
719 MacPhee, R. D. 2015. Ancient proteins resolve the evolutionary history of Darwin's
720 South American ungulates. *Nature*, *522*(7554), 81-84.
721 Zhang B, Tong H. 2024. The comparative anatomy of the petrosal bone and bony
722 labyrinth of four small-sized deer. *The Anatomical Record* 307:566–580. DOI:
723 10.1002/ar.25303.

Table 1(on next page)

Petrosal specimens examined in the study

Specimen #	Taxon	Locality	Age	Left or right	Bony Labyrinth	Stapes
NMB.San.15063	*Anchitherium aurelianense*	Sansan, Gers France	Astaracian (MN 6)	Right	No (no contrast)	No
NMB.A.Mo.655	*Hipparion depereti*	Montredon, Occitanie, France	Vallesian (MN 10)	Left	Yes	No
NMB.Ccd.3	*Hipparion concudense*	Concud 3, Teruel, Spain	Turolian (MN 12)	Left	Yes	Yes
NMB.V.A.2753	*Equus stenonis*	Valdarno, Tuscany, Italy	Villafranchian (MN17)	Left	Yes	Yes
NMB.Se.141	*Equus senezensis*	Senèze, Alpes-de-Haute-Provence, France	Villafranchian (MN 17)	Left	Yes	Yes
NMB.Se.141	*Equus senezensis*	Senèze, Alpes-de-Haute-Provence, France	Villafranchian (MN 17)	Right	Yes	No
NMB.Se.554	*Equus senezensis*	Senèze, Alpes-de-Haute-Provence, France	Villafranchian (MN 17)	Left	Yes	No

1 Table 1. Petrosal specimens examined in the study.
2

Figure 1

Map of fossil sites for equid specimens in this study (right) and the corresponding stratigraphic and biostratigraphic ages of those sites (left).

ELMMZ= European Large Mammal Mega-Zone, MNQ= Mammal Neogene/Quaternary Biostratigraphic Stage. Silhouettes from Phylopic made by Julian Bayona.

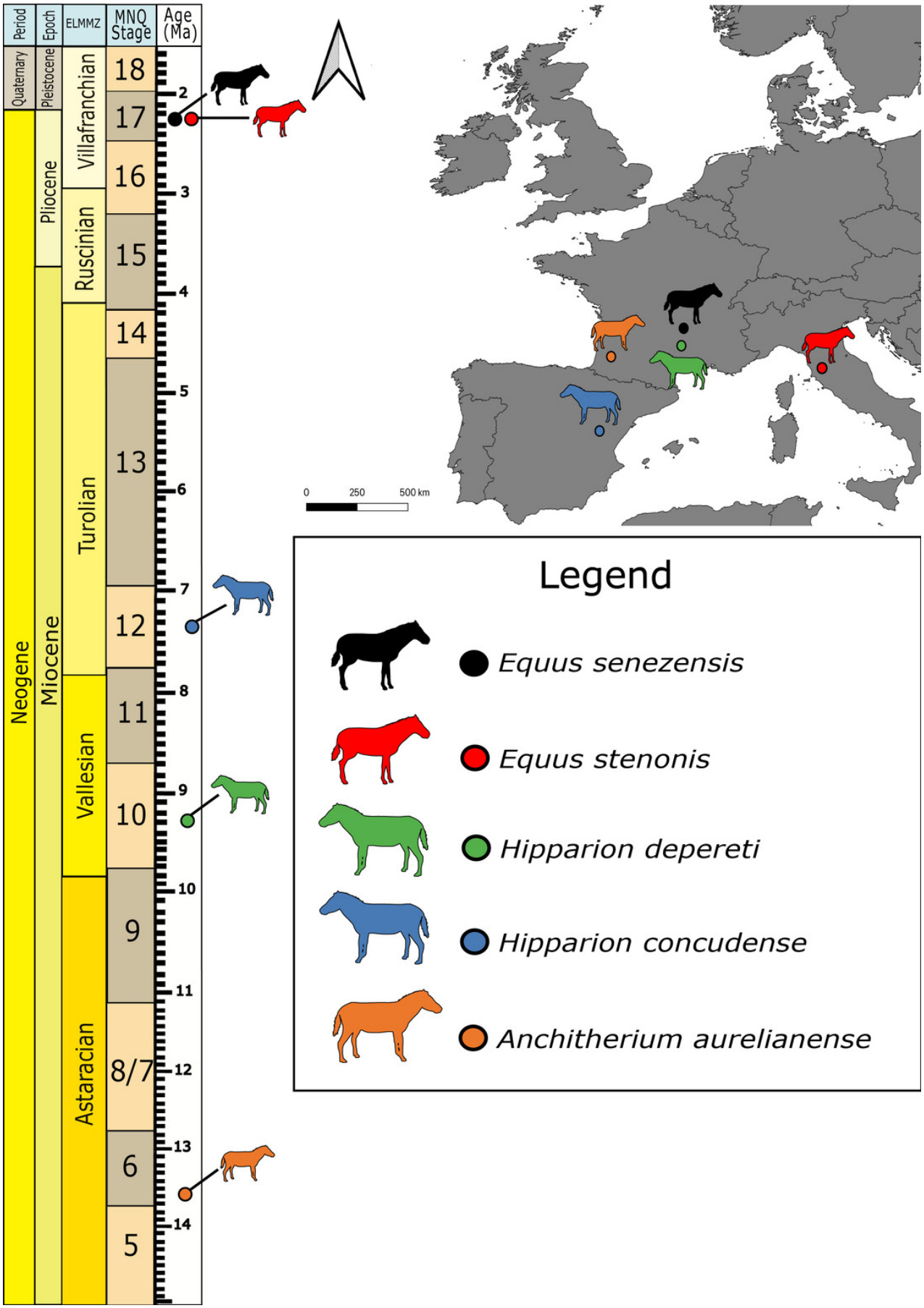
Period
Epoch
ELMMZ
MNQ Stage
Age (Ma)
Quaternary
Pleistocene
Villafranchian
18
17
16
Pliocene
Ruscinian
15
14
Neogene
Miocene
Turolian
13
12
Vallesian
11
10
9
Astaracian
8/7
6
5
2
3
4
5
6
7
8
9
10
11
12
13
14
0
250
500 km
Legend
Equus senezensis
Equus stenonis
Hipparion depereti
Hipparion concudense
Anchitherium aurelianense

Figure 2

Right petrosal (NMB.San.15063) of *Anchitherium aurelianense* from Sansan.

(A) Ventrolateral view. (B) Ventromedial view. (C) Anterior view. (D) dorsomedial view. (E) Dorsolateral view. The specimen has been reversed from the original for comparison.

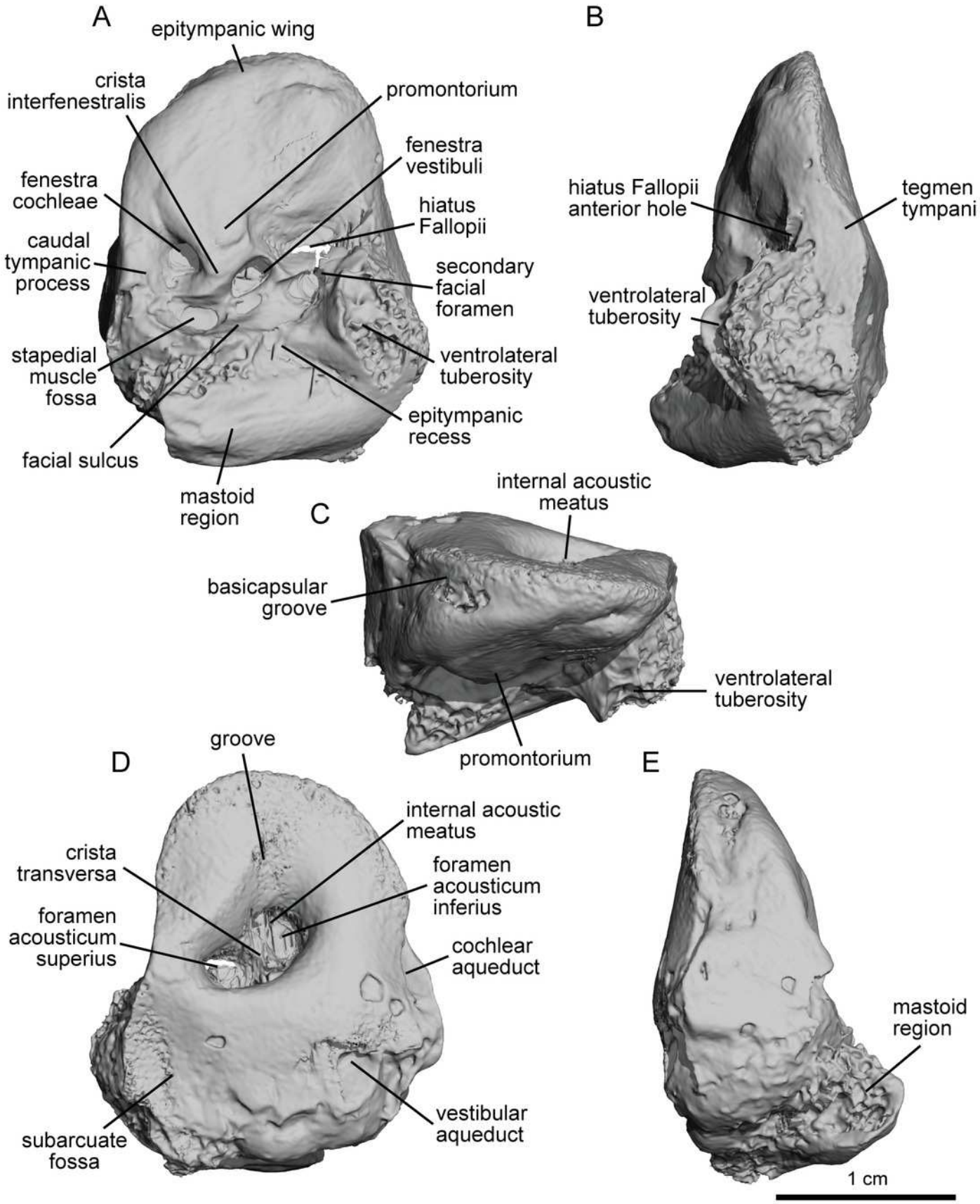
A
epitympanic wing
crista interfenestralis
promontorium
fenestra vestibuli
fenestra cochleae
hiatus Fallopii
caudal tympanic process
secondary facial foramen
stapedial muscle fossa
ventrolateral tuberosity
epitympanic recess
facial sulcus
mastoid region
B
hiatus Fallopii anterior hole
tegmen tympani
ventrolateral tuberosity
C
internal acoustic meatus
basicapsular groove
ventrolateral tuberosity
promontorium
D
groove
internal acoustic meatus
crista transversa
foramen acousticum inferius
foramen acousticum superius
cochlear aqueduct
subarcuate fossa
vestibular aqueduct
E
mastoid region
1 cm

Figure 3

Left petrosal (NMB.A.Mo.655) of *Hipparion depereti* from Montredon.

(A) Ventrolateral transparent view. (B) Ventrolateral opaque view. (C) dorsolateral view. (D) Anterior view. (E) Dorsomedial view. (F) Ventromedial view.

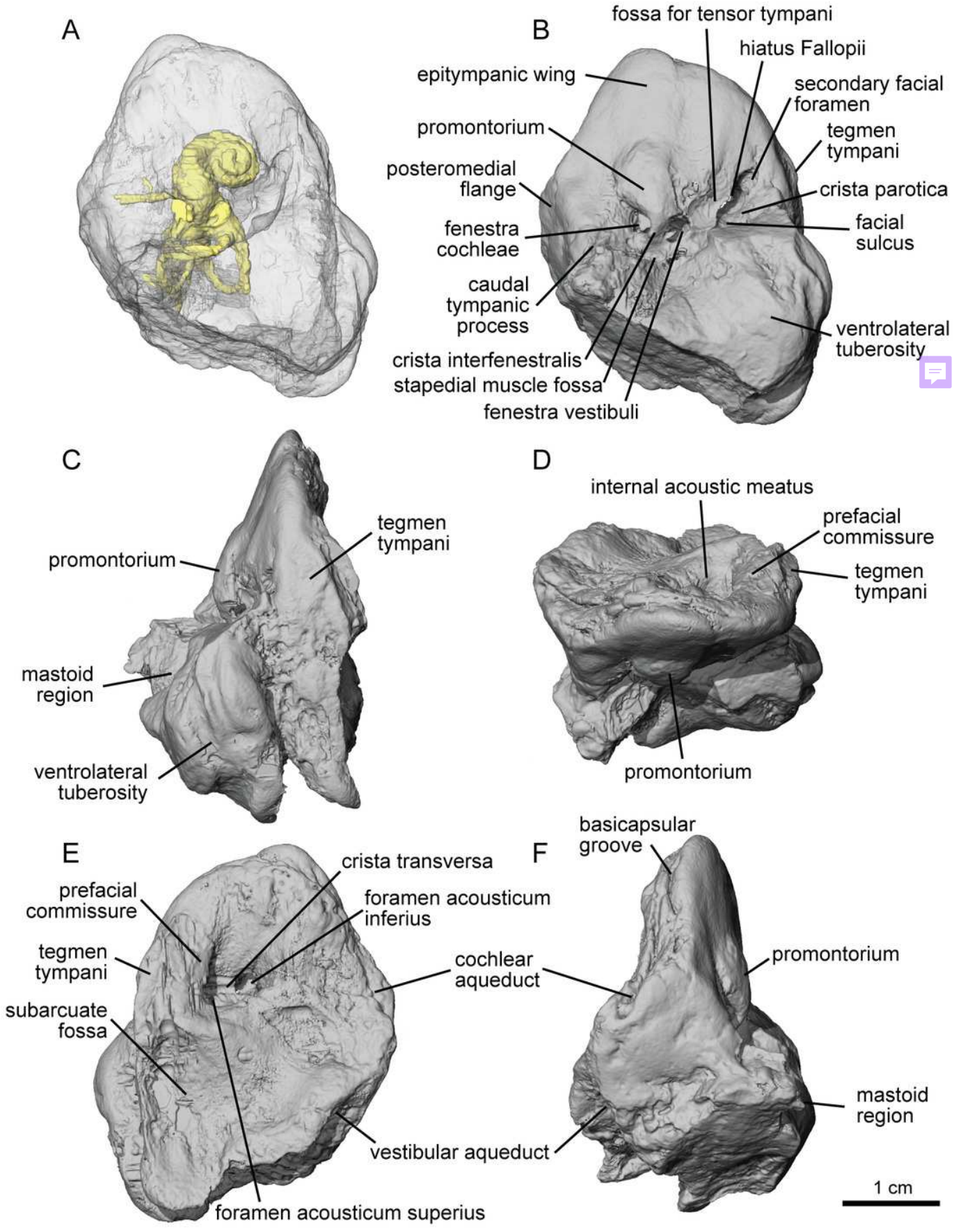
A
B
fossa for tensor tympani
hiatus Fallopii
epitympanic wing
secondary facial foramen
promontorium
tegmen tympani
posteromedial flange
crista parotica
fenestra cochleae
facial sulcus
caudal tympanic process
ventrolateral tuberosity
crista interfenestralis
stapedial muscle fossa
fenestra vestibuli
C
tegmen tympani
promontorium
mastoid region
ventrolateral tuberosity
D
internal acoustic meatus
prefacial commissure
tegmen tympani
promontorium
E
crista transversa
prefacial commissure
foramen acousticum inferius
tegmen tympani
cochlear aqueduct
subarcuate fossa
vestibular aqueduct
foramen acousticum superius
F
basicapsular groove
promontorium
mastoid region
1 cm

Figure 4

Endocast of bony labyrinth of *Hipparion depereti* (NMB.A.Mo.655) from Montredon.

(A) Anterior view. (B) Posterior view. (C) Lateral view. (D) Dorsal view.

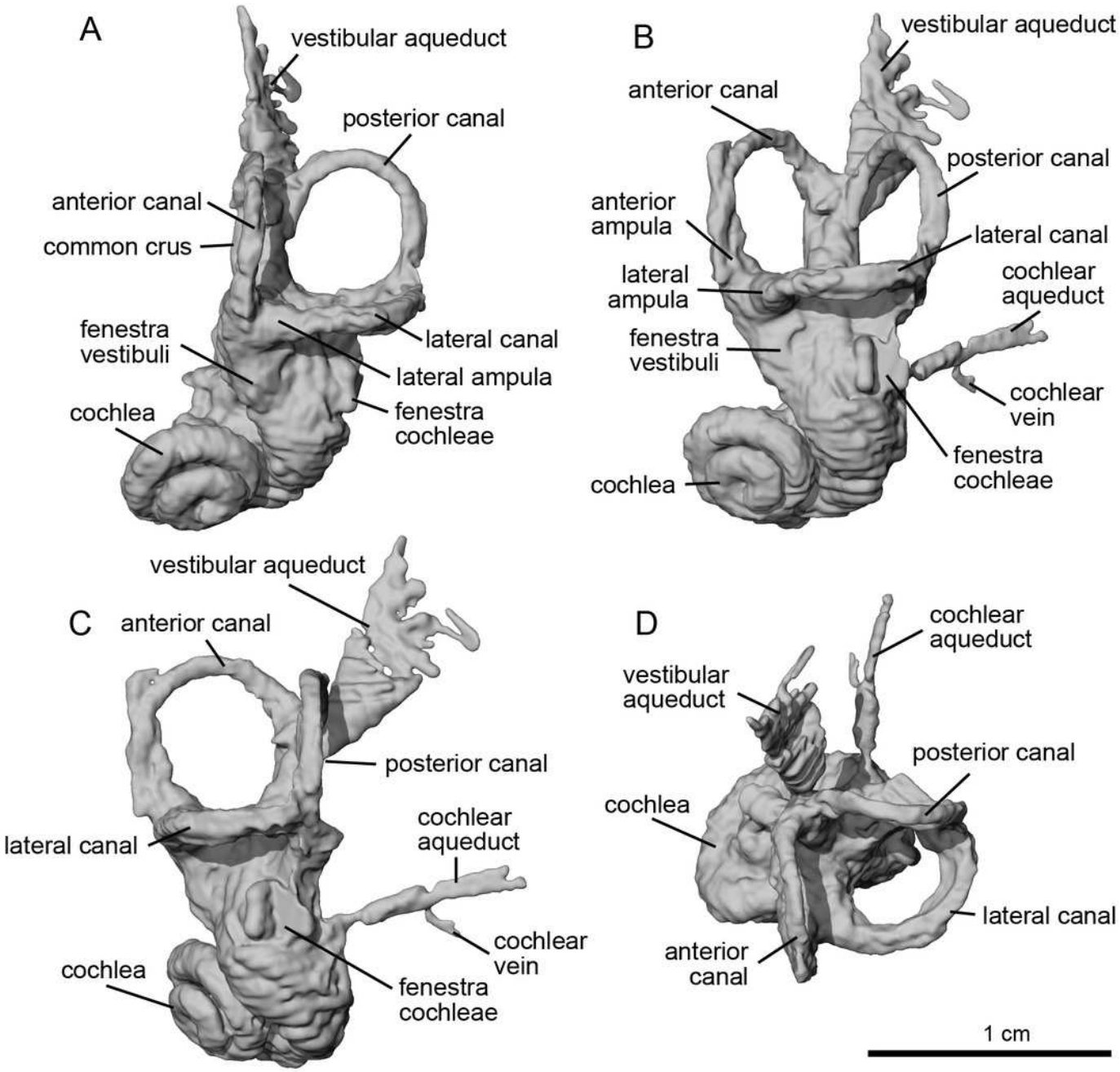

Figure 5

Left petrosal (NMB.Ccd.3) of *Hipparion concudense* from Concud3.

(A) Ventrolateral transparent view. (B) Ventrolateral opaque view. (C) dorsolateral view. (D) Anterior view. (E) Dorsomedial view. (F) Ventromedial view.

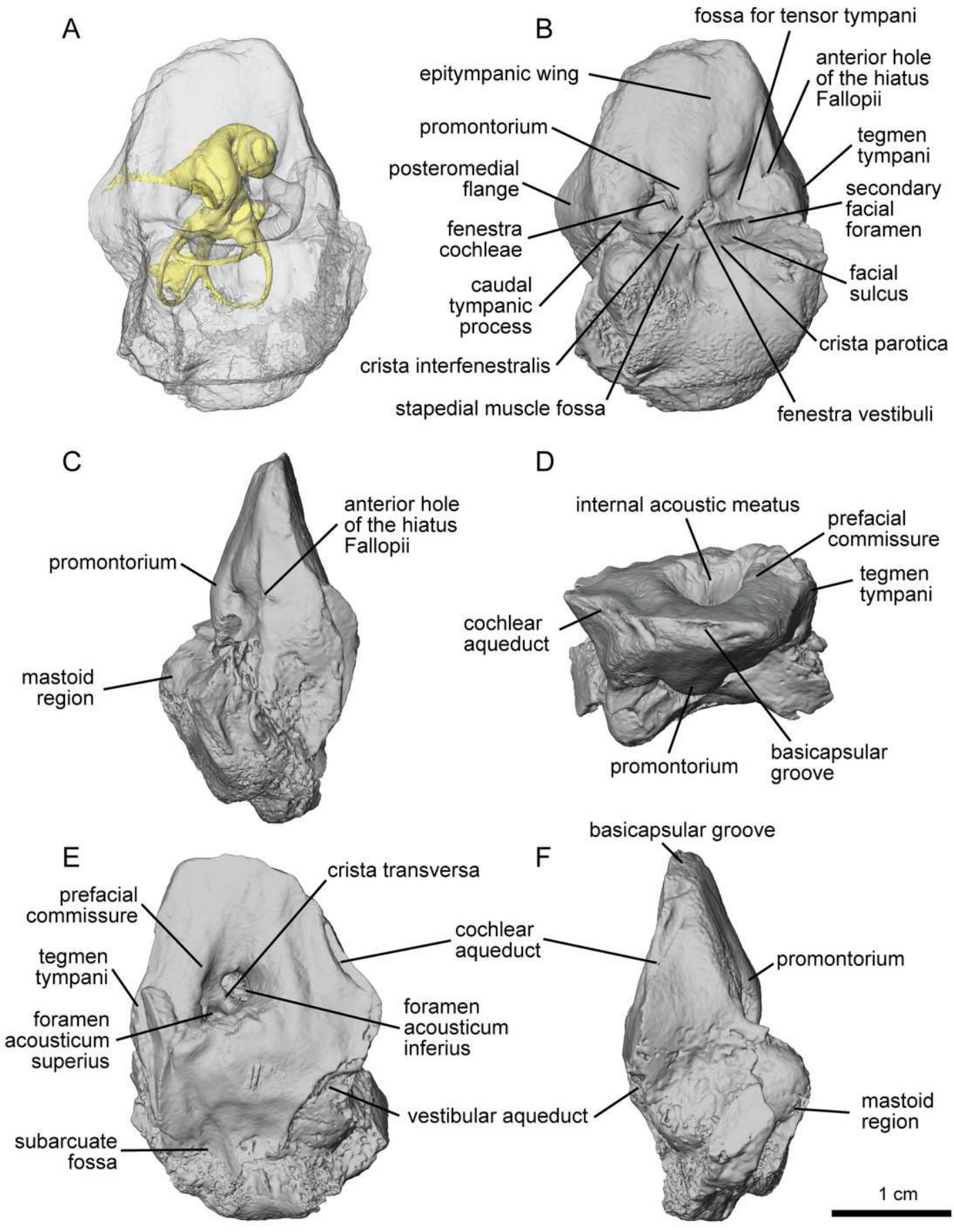
A
B
fossa for tensor tympani
epitympanic wing
anterior hole of the hiatus Fallopii
promontorium
tegmen tympani
posteromedial flange
secondary facial foramen
fenestra cochleae
facial sulcus
caudal tympanic process
crista parotica
crista interfenestralis
stapedial muscle fossa
fenestra vestibuli
C
D
anterior hole of the hiatus Fallopii
promontorium
internal acoustic meatus
prefacial commissure
tegmen tympani
cochlear aqueduct
mastoid region
promontorium
basicapsular groove
E
F
basicapsular groove
crista transversa
prefacial commissure
cochlear aqueduct
tegmen tympani
promontorium
foramen acousticum inferius
foramen acousticum superius
vestibular aqueduct
mastoid region
subarcuate fossa
1 cm

Figure 6

Endocast of the bony labyrinth of *H. concudense* (NMB.Ccd.3) from Concud3.

(A) Anterior view. (B) Posterior view. (C) Lateral view. (D) Dorsal view.

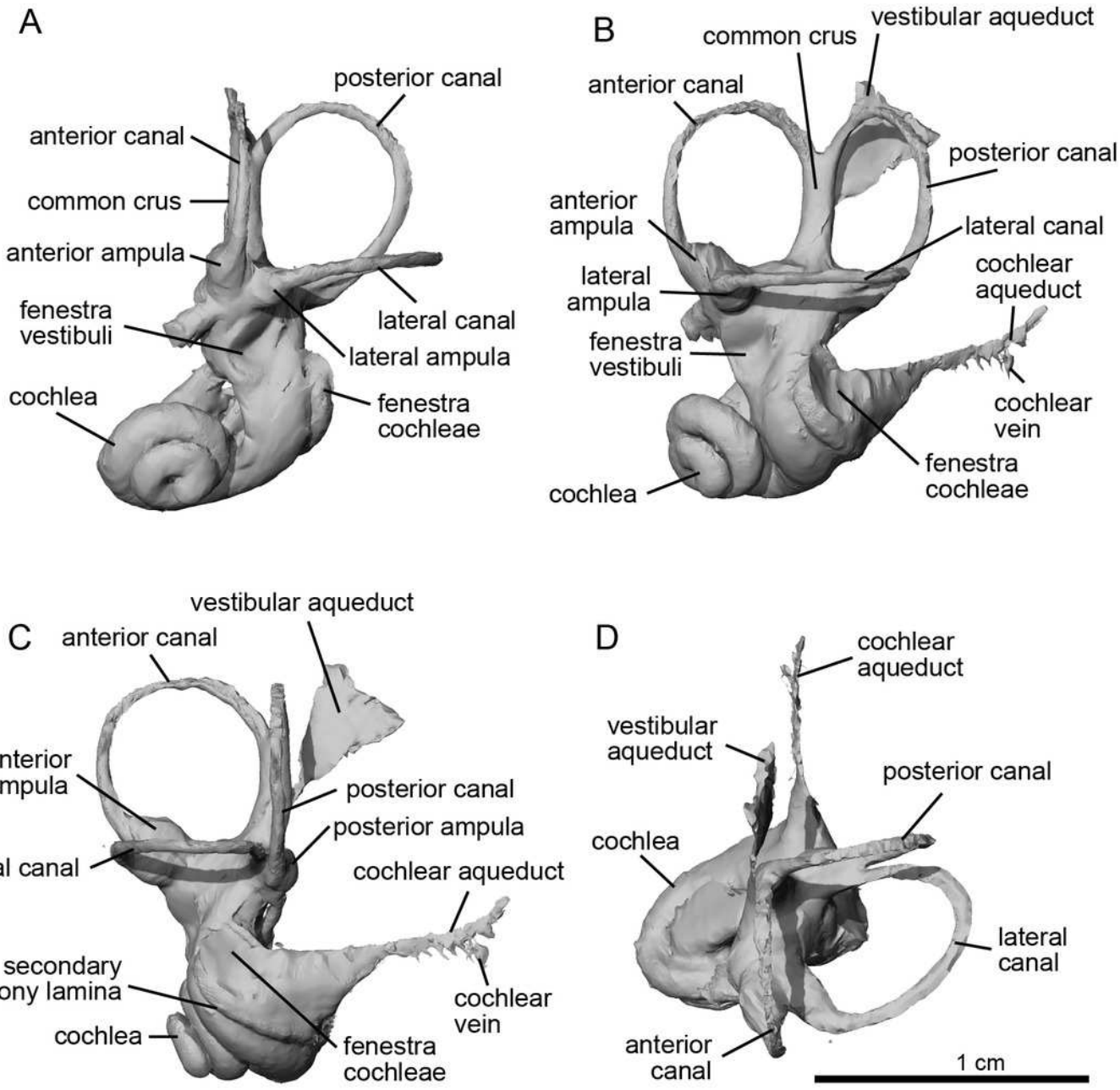

Figure 7

Left stapes preserved within the petrosals.

(A) *Hipparion concudense* (NMB.Ccd.3). (B) *Equus stenonis* (NMB.V.A.2753). (C) *Equus senezensis* (NMB.Se.141). Abbreviations: bs, *basis stapedis*; cas, *crus anterius stapedis*; cps, *crus posterius stapedis*; fi, *foramen intercrurale*; pms, *processus muscularis stapedis*.

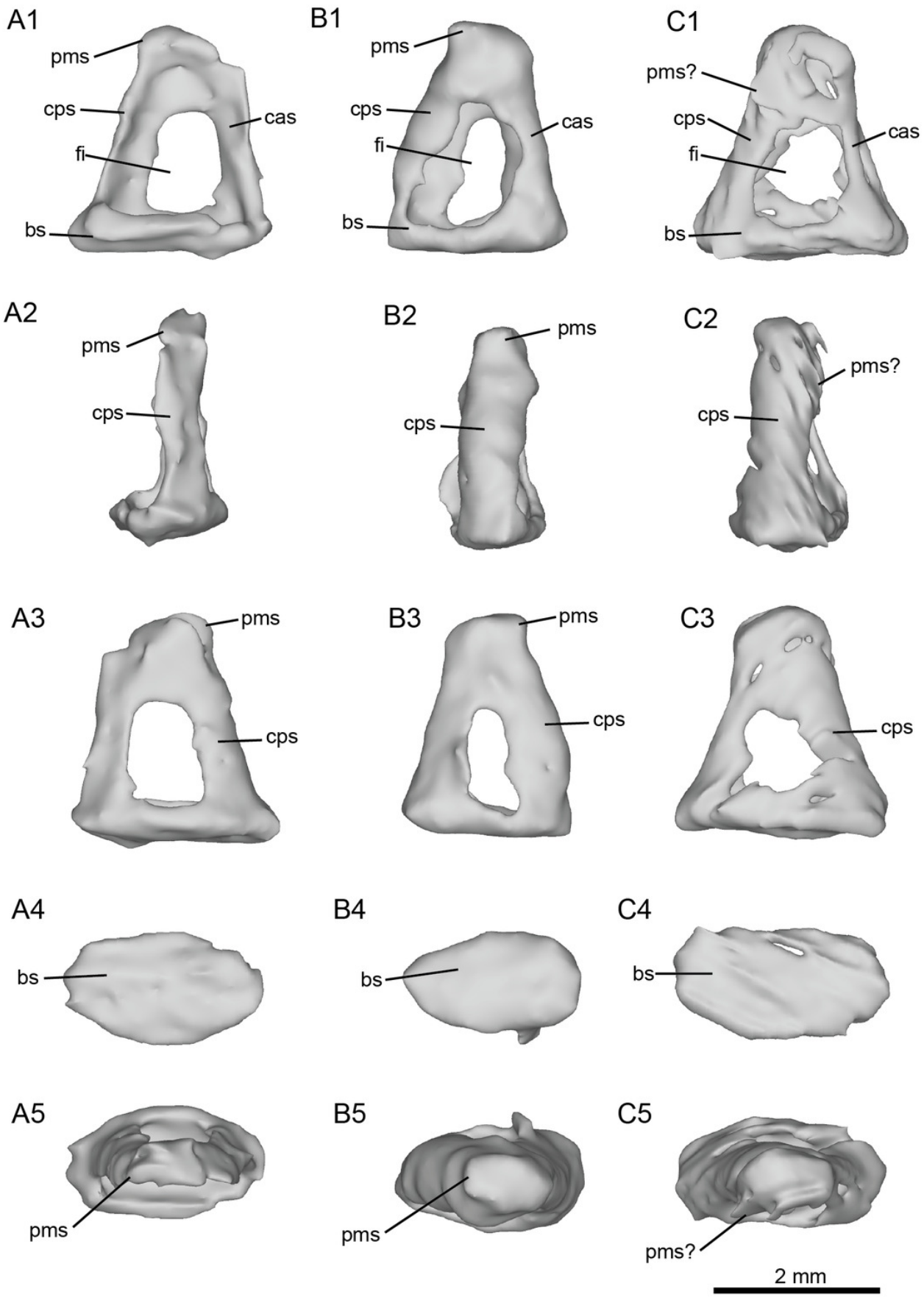
A1
pms
cps
cas
fi
bs
B1
pms
cps
cas
fi
bs
C1
pms?
cps
cas
fi
bs
A2
pms
cps
B2
pms
cps
C2
pms?
cps
A3
pms
cps
B3
pms
cps
C3
cps
A4
bs
B4
bs
C4
bs
A5
pms
B5
pms
C5
pms?
2 mm

Figure 8

Left petrosal (NMB.V.A.2753) of *Equus stenonis* from Valdarno.

(A) Ventrolateral transparent view. (B) Ventrolateral opaque view. (C) dorsolateral view. (D) Anterior view. (E) Dorsomedial view. (F) Ventromedial view.

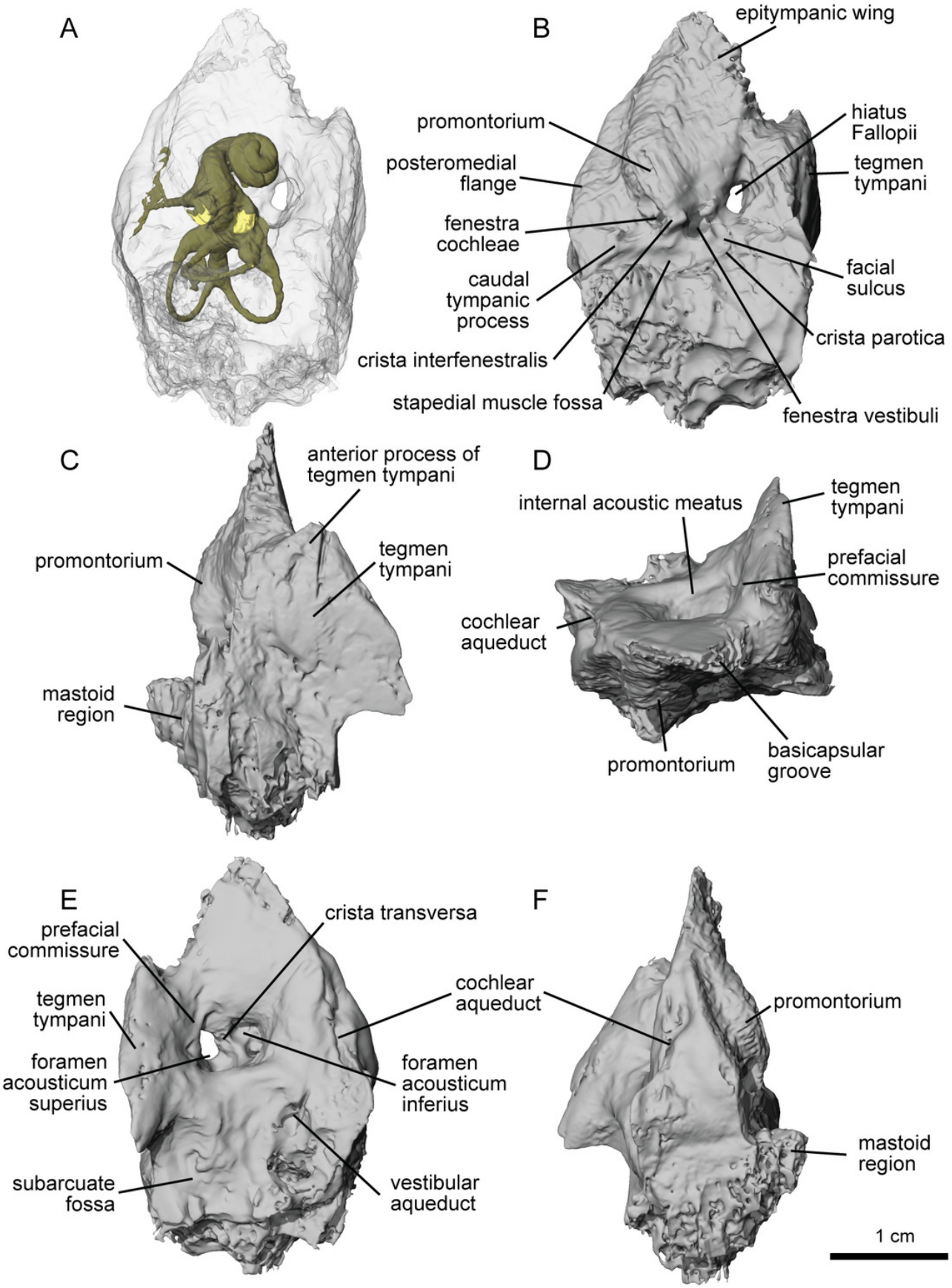
A
B
epitympanic wing
promontorium
posteromedial flange
fenestra cochleae
caudal tympanic process
crista interfenestralis
stapedial muscle fossa
hiatus Fallopii
tegmen tympani
facial sulcus
crista parotica
fenestra vestibuli
C
anterior process of tegmen tympani
promontorium
tegmen tympani
mastoid region
D
internal acoustic meatus
tegmen tympani
prefacial commissure
cochlear aqueduct
promontorium
basicapsular groove
E
crista transversa
prefacial commissure
tegmen tympani
foramen acousticum superius
subarcuate fossa
cochlear aqueduct
foramen acousticum inferius
vestibular aqueduct
F
promontorium
mastoid region
1 cm

Figure 9

Endocast of the bony labyrinth of *E. stenonis* (NMB.V.A.2753) from Valdarno.

(A) Anterior view. (B) Posterior view. (C) Lateral view. (D) Dorsal view.

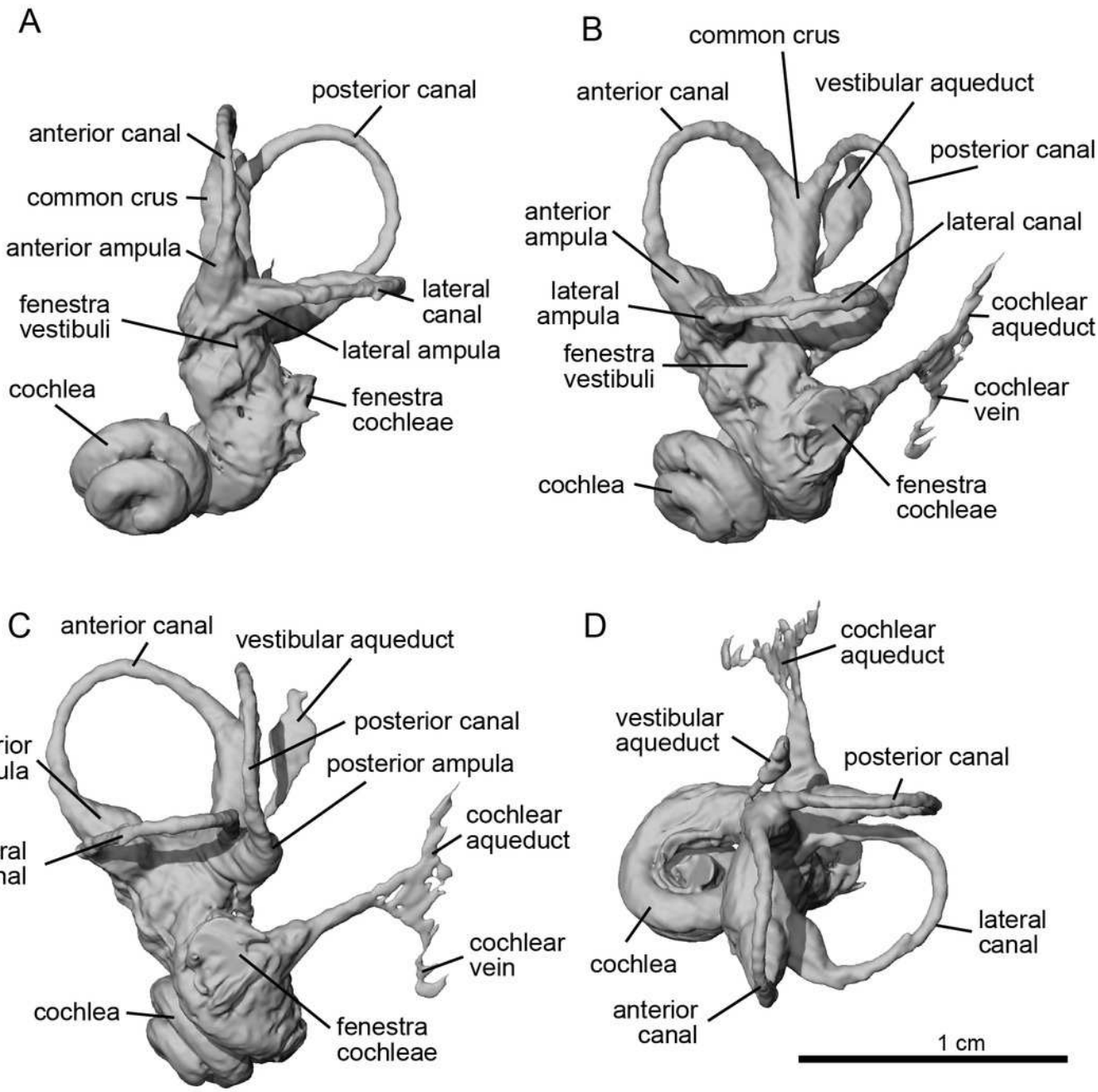

Figure 10

Left petrosal (NMB.Se.141) of *Equus senezensis* from Senèze.

(A) Ventrolateral transparent view. (B) Ventrolateral opaque view. (C) dorsolateral view. (D) Anterior view. (E) Dorsomedial view. (F) Ventromedial view.

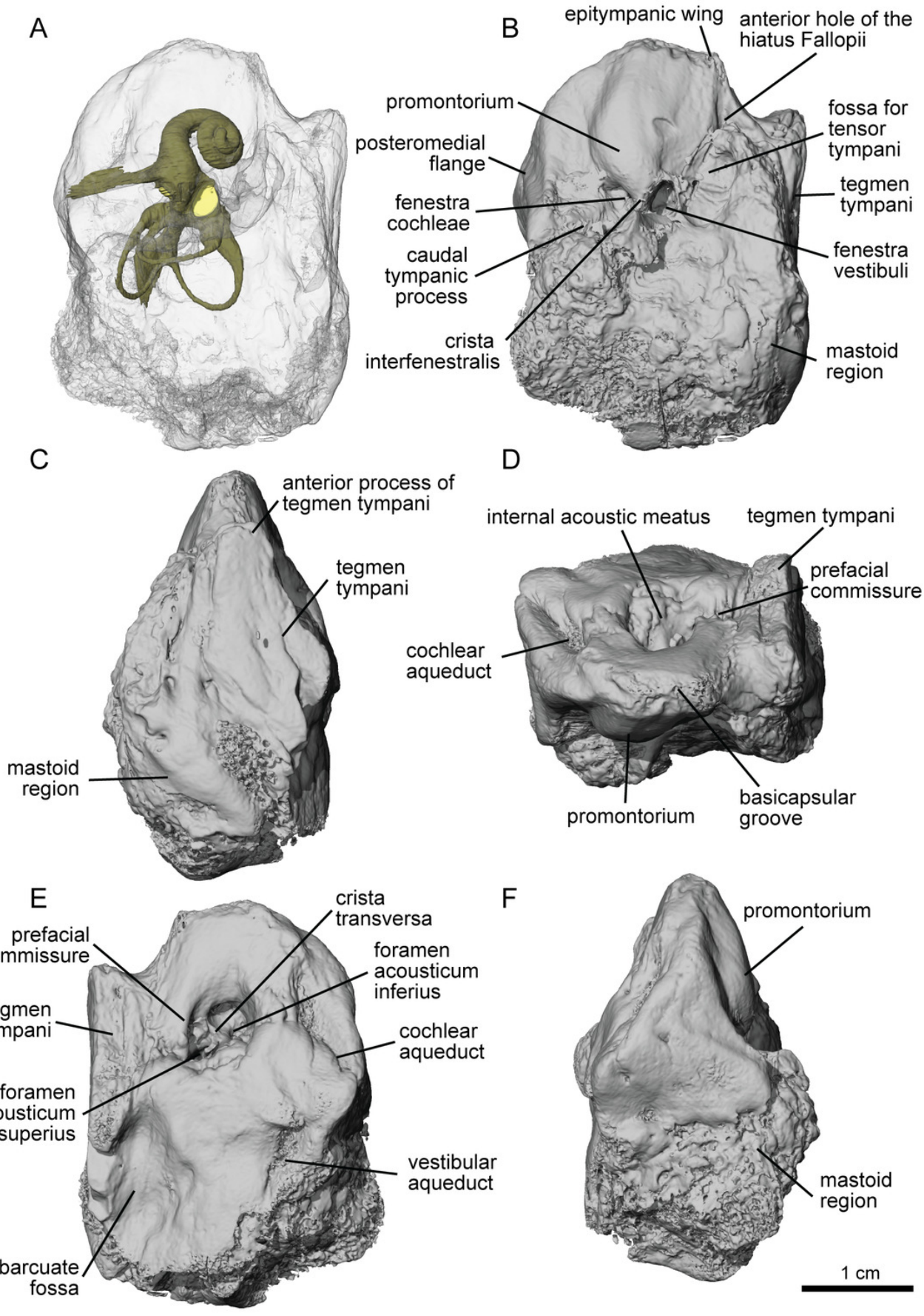
A
B
epitympanic wing
anterior hole of the hiatus Fallopii
promontorium
fossa for tensor tympani
posteromedial flange
tegmen tympani
fenestra cochleae
fenestra vestibuli
caudal tympanic process
crista interfenestralis
mastoid region
C
anterior process of tegmen tympani
tegmen tympani
mastoid region
D
internal acoustic meatus
tegmen tympani
prefacial commissure
cochlear aqueduct
promontorium
basicapsular groove
E
crista transversa
prefacial commissure
foramen acousticum inferius
tegmen tympani
cochlear aqueduct
foramen acousticum superius
vestibular aqueduct
subarcuate fossa
F
promontorium
mastoid region
1 cm

Figure 11

Left petrosal (NMB.Se.554) of *Equus senezensis* from Senèze.

(A) Ventrolateral transparent view. (B) Ventrolateral opaque view. (C) dorsolateral view. (D) Anterior view. (E) Dorsomedial view. (F) Ventromedial view.

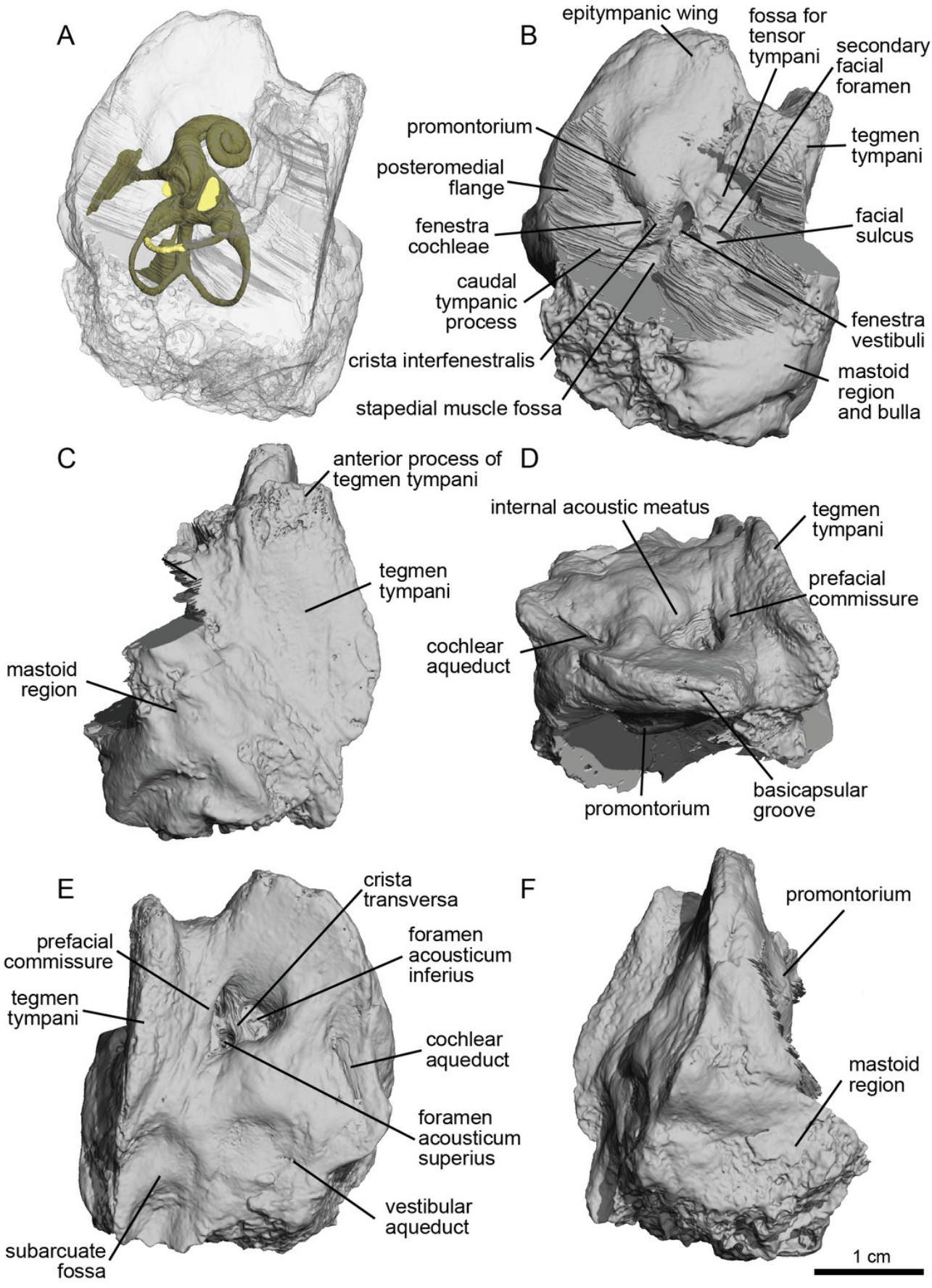
A
B
epitympanic wing
fossa for tensor tympani
secondary facial foramen
promontorium
tegmen tympani
posteromedial flange
facial sulcus
fenestra cochleae
caudal tympanic process
fenestra vestibuli
crista interfenestralis
mastoid region and bulla
stapedial muscle fossa
C
anterior process of tegmen tympani
tegmen tympani
mastoid region
D
internal acoustic meatus
tegmen tympani
prefacial commissure
cochlear aqueduct
promontorium
basicapsular groove
E
crista transversa
prefacial commissure
foramen acousticum inferius
tegmen tympani
cochlear aqueduct
foramen acousticum superius
vestibular aqueduct
subarcuate fossa
F
promontorium
mastoid region
1 cm

Figure 12

Endocast of the bony labyrinth of *Equus senezensis* (NMB.Se.141) from Senèze.

(A) Anterior view. (B) Posterior view. (C) Lateral view. (D) Dorsal view.

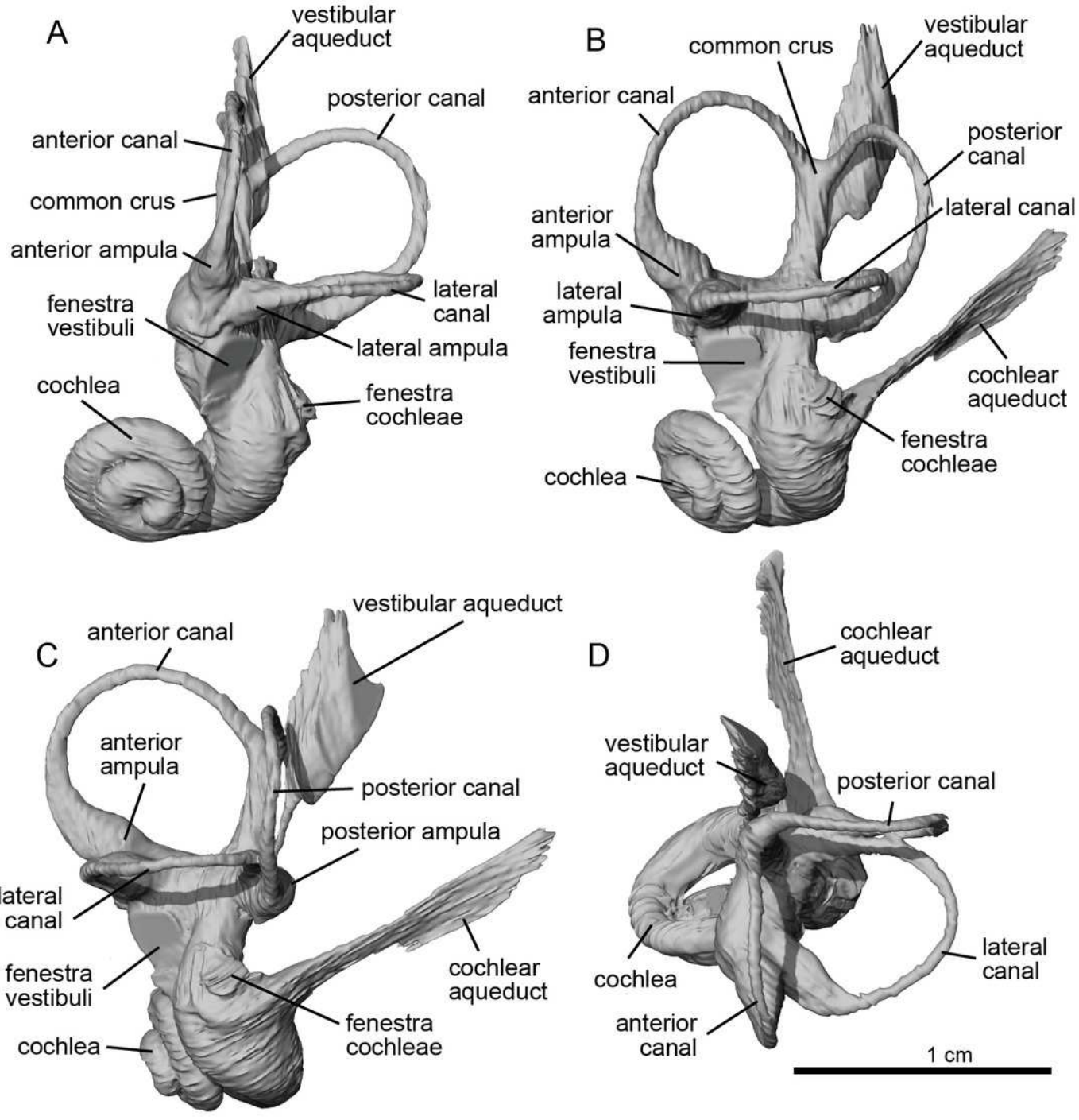
A
vestibular aqueduct
posterior canal
anterior canal
common crus
anterior ampula
lateral canal
fenestra vestibuli
lateral ampula
cochlea
fenestra cochleae
B
common crus
vestibular aqueduct
anterior canal
posterior canal
lateral canal
anterior ampula
lateral ampula
fenestra vestibuli
cochlear aqueduct
fenestra cochleae
cochlea
C
vestibular aqueduct
anterior canal
anterior ampula
posterior canal
posterior ampula
lateral canal
cochlear aqueduct
fenestra vestibuli
fenestra cochleae
cochlea
D
cochlear aqueduct
vestibular aqueduct
posterior canal
lateral canal
cochlea
anterior canal
1 cm

Figure 13

Endocast of the bony labyrinth of *Equus senezensis* (NMB.Se.554) from Senèze.

(A) Anterior view. (B) Posterior view. (C) Lateral view. (D) Dorsal view.

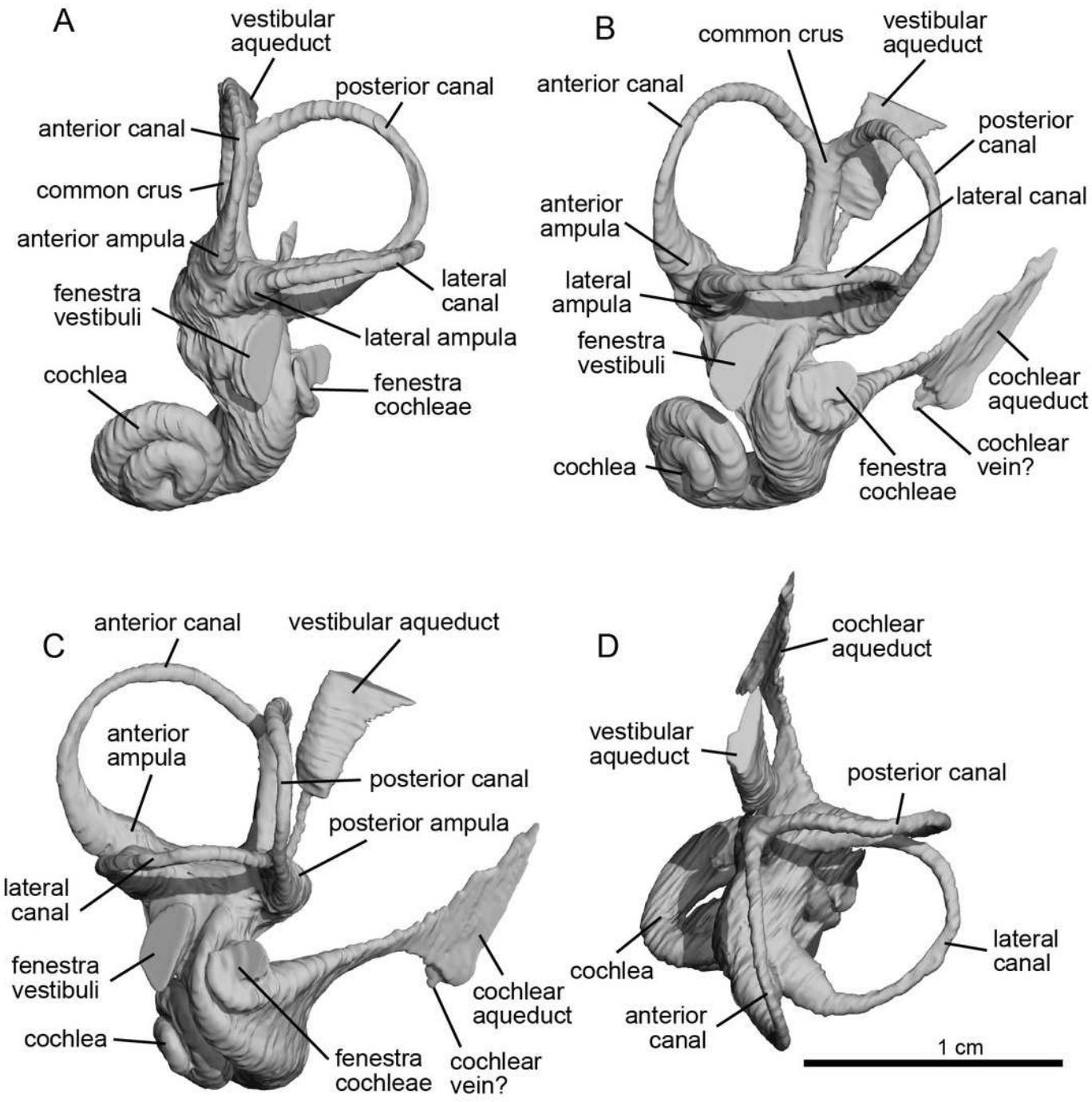

Figure 14

Phylogeny of the studied Equidae based on ear region characters.

Single most-parsimonious tree of 25 steps (CI=0.88, HI=0.12, RI=0.82) with *Hyopsodus* considered as outgroup, obtained by an exhaustive search with a parsimony algorithm in PAUP*4. Apomorphies are indicated as “character number:state” at nodes. Silhouettes of horses from Phylopic made by Julian Bayona.

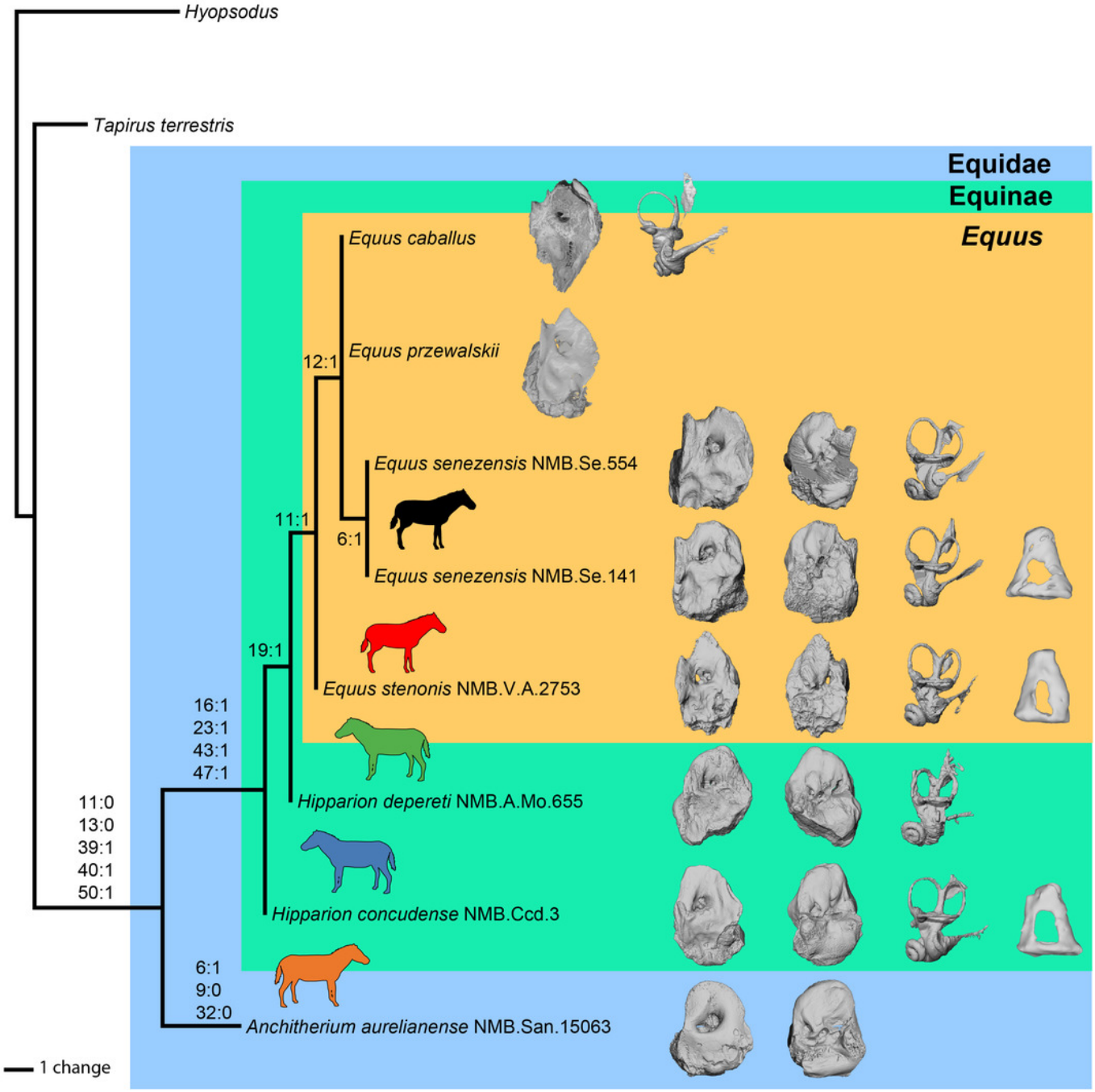
Hyopsodus
Tapirus terrestris
Equidae
Equinae
Equus
Equus caballus
Equus przewalskii
Equus senezensis NMB.Se.554
Equus senezensis NMB.Se.141
Equus stenonis NMB.V.A.2753
Hipparion depereti NMB.A.Mo.655
Hipparion concudense NMB.Ccd.3
Anchitherium aurelianense NMB.San.15063
12:1
11:1
6:1
19:1
16:1
23:1
43:1
47:1
11:0
13:0
39:1
40:1
50:1
6:1
9:0
32:0
1 change